Sede Amministrativa: Università degli Studi di Padova

Dipartimento di Biologia

SCUOLA DI DOTTORATO DI RICERCA IN: BIOSCIENZE E BIOTECNOLOGIE
INDIRIZZO: BIOLOGIA CELLULARE
CICLO: XXVIII

STRUCTURAL AND FUNCTIONAL CHARACTERIZATION OF A-B TOXINS: DIPHTHERIA TOXIN AND CLOSTRIDIAL NEUROTOXINS

Direttore della Scuola: Ch.mo Prof. Paolo Bernardi
Coordinatore d'indirizzo: Ch.mo Prof. Paolo Bernardi
Supervisore: Ch.mo Prof. Cesare Montecucco

Dottoranda: Oneda Leka

Alla mia grande famiglia

TABLE OF CONTENTS

Pubblications list

Acknowledgements

ABBREVIATIONS

BoNTs: Botulinum NeuroToxins

TeNT: Tetanus neuroToxin

DT: Diphtheria Toxin

DT-A: Diphtheria Toxin fragment A

DT-B: Diphtheria Toxin fragment B

VAMP: Vesicle Associated Membrane Protein

SNAP-25: SyNaptosome Associated Protein 25

SUMMARY

I performed my doctorate research activity studying three important human pathogens that are A-B toxins: Diphtheria Toxin (DT), Tetanus Neurotoxin (TeNT) and Botulinum neurotoxins (BoNTs), the etiologic agents of diphtheria, tetanus and botulism respectively. In terms of structural organization these toxins consist of three domains, which are termed L chain (the N-terminal catalytic domain), HN (the transmembrane domain), and HC (the C-terminal binding domain). These domains are closely related to the common four step mechanism of action: membrane binding mediated by HC, endocytosis, membrane translocation mediated by HN and L-chain mediated substrate modification.

I studied the conformational change of diphtheria toxin at acidic pH. DT includes a T domain which is known to mediate the pH-dependent membrane translocation, by forming a channel through which the catalytic domain crosses the endocytic vesicle membrane. To date no structural data are available about the pore/channel formed by the T domain, nor is known if it is monomeric or oligomeric. I have performed biochemical and structural studies to characterize the T domain of DT. The T domain is also considered a prospective anti-cancer agent for the targeted delivery of cytotoxic therapy to cancer cells. I obtained the crystal structure of DT in the presence of lipid bicelles (which simulate the endocytic vesicle membrane) and grown at pH 5.5, pH that mimics the acidic environment where translocation takes place. The reported structure throws lights on the initial event of this process, the destabilization of the three α-helices present at the bottom of the toxin (Leka *et al.*, 2014).

I then worked on a project which aimed to unravel the three dimensional structure of tetanus neurotoxin by crystallization studies. Because TeNT is considered "uncrystallizable" I focused on the use of antibody fragments (Fabs) as crystallization chaperons to aid the structural determination. Native gel analysis and size exclusion chromatography showed the formation of a stable complex *in vitro* between TeNT and the relative Fabs. Several crystallization experiments were carried out by high throughput crystallization screens.

Further, I performed functional analysis on the trafficking of botulinum neurotoxin at the neuromuscular junction (NMJ). I expressed the binding domains of different BoNT serotypes, which are both necessary and sufficient for binding to the neuronal surface and internalization. The two step purifications, chromatography and gel filtration, were sufficient to yield purifications of each binding domain to >90% purity. Using cerebellum granular neurons (CGNs), I tested their functionality and specificity. I performed also *in vivo* assays in order to analyze their distribution along the NMJ. The data from fluorescence analysis show high specificity of these binding domains at the NMJ, and a different staining between different BoNT serotypes, reflecting their different time of intoxication, and perhaps a different pathway of vesicular trafficking.

RIASSUNTO

Ho effettuato la mia attività di ricerca studiando tre importanti patogeni umani, che sono tossine di tipo A-B: la tossina difterica (DT), la neurotossina tetanica (TeNT) e le neurotossine botuliniche (BoNTs), gli agenti eziologici di difterite, tetano e botulismo, rispettivamente. In termini di organizzazione strutturale queste tossine sono costituite da tre domini: il dominio catalitico (LH), il dominio di translocazione (HN) e il dominio di legame (HC). Questa organizzazione dei domini è strettamente correlata al loro comune meccanismo d'azione che comprende: il legame alla membrane cellulare mediato dal HC, la traslocazione del dominio catalitico nel citoplasma mediata dal canale di permeazione formato dal HN. Ho studiato il cambiamento conformazionale della tossina difterica a pH acido. DT include un dominio di translocazione (dominio T), che forma il canale attraverso il quale il dominio catalitico attraversa la membrana della vescicola endosomica. Fino ad oggi non ci sono dati strutturali che riguardano il canale formato dal dominio T, non si sa neanche se è un monomero o oligomero. Ho eseguito studi biochimici e strutturali per caratterizzare il dominio T di DT. Il dominio T è anche considerato un agente anti-cancro nelle terapie mirate contro le cellule tumorali. Ho ottenuto la struttura tridimensionale della tossina difterica in presenza di doppi strati lipidici (che simulano la membrana della vescicola endosomica) ed in condizioni di pH 5,5 (pH corrispondente all'ambiente acido in cui avviene la il processo di traslocazione). La struttura riportata getta luci sull'evento iniziale di questo processo, la destabilizzazione di tre alfa-eliche presenti nella parte inferiore della tossina (Leka *et al.*, 2014).

Ho poi lavorato su un progetto che mirava a caratterizzare la struttura tridimensionale della tosssina tetanica. Poiché la cristallizzazione di questa tossina risulta d'essere molto difficile, mi sono concentrata sull'utilizzo di frammenti di anticorpi (Fab) come tools per aiutare la determinazione strutturale. Analisi da gel nativo e da cromatografia ad esclusione mostrano la formazione di un complesso stabile *in vitro* tra la tossina ed i relativi Fab. Diversi esperimenti di cristallizzazione sono stati eseguiti, e per il momento non abbiamo ancora informazioni strutturali sulla tossina.

Inoltre, ho studiato anche la localizzazione ed il processo di internalizzazione delle tossine botuliniche a livello della giunzione neuromuscolare (NMJ). Ho espresso i domini di legame di diversi sierotipi di tossine botuliniche, domini che sono necessari e sufficienti per il legame alla superficie dei neuroni. I domini di legame sono stati purificati utilizzando cromatografia di affinità e per esclusione, ottendo alla fine una purezza > 90% . Utilizzando i neuroni granulari di cervelletto (CGN), ho testato la loro funzionalità e specificità. Questi domini sono stati iniettati *in vivo* al fine di analizzare la loro localizzazione a livello della giunzione neuromuscolare. I dati ottenuti con analisi di microscopia confocale ed a fluorescenza mostrano che questi domini si localizzano proprio a livello della giunzione muscolare. Nelle marcature si osserva anche una colorazione diversa tra i diversi sierotipi BoNT, e questo risultato riflette il diverso tempo di intossicazione tra i vari serotipi di tossine botuliniche, e forse anche una diversa localizzazione in diverse vescicole endosomiche.

INTRODUCTION

1. Bacterial protein toxins

Toxins are virulence factors produced by pathogenic bacteria to colonise and/or to multiply within the animal host. Bacterial protein toxins have reached an amazing level of specialisation and adaptation to the targeted organism or cell type in order to achieve an efficient subversion of host cell function. The study of host-pathogen interactions has offered scientists different strategies that have resulted from the evolutionary race between eukaryotic cells and competing microorganisms. The result of this evolutionary pressure was the identification of several virulence factors/proteins that interfere with fundamental cellular processes (Schiavo *et al.,* 2001; Kahn *et al.,* 2002). The biochemical analysis of these molecules and the characterization of their cellular mechanism of action have yielded several targets for vaccine development and therapeutic intervention.

1.1 A-B toxins

A huge number of proteins produced by bacterial pathogens are highly toxic to mammalian cells due to their ability to attack/destroy essential cellular metabolic and/or signal transduction pathways. These toxic proteins mostly belong to the A-B toxin family (Barth *et al.,* 2004). A-B toxins are composed by two structurally and functionally distinctive protomers: A and B. The protomer B is generated only after proteolysis of the precursor molecules. It mediates the binding to a specific receptor on the host cell membrane. The B protomer-receptor complex then acts as a docking platform that subsequently translocates the enzymatic A component into the cytosol via acidified vesicular compartments. Once inside the cytosol, the A protomer can inhibit normal cell function. Not only these toxins are important virulence factors, but also they are useful biological tools for studying several cellular functions and delivering heterologous proteins into endosomal, as well as cytosolic compartments. Usually, an A-B toxin is synthesized and secreted from the bacteria pathogen as an inactive form. The inactive precursor is then activated through a proteolytic cleavage performed by a host or pathogen protease at a region between two cysteine residues. The cleavage results in a di-chain toxin molecule with the protomer A and B linked by a disulphide bond. Some toxins, such as anthrax toxin, diphtheria toxin, and Clostridial neurotoxins traffic to vesicular compartments, where acidification triggers conformational change on the B protomer that forms a protein conductive channel/pore on the membrane through which it

translocates A protomer. Instead, other A-B toxins, including shiga toxin, cholera toxin, exotoxin A will travel through a different transport pathway to arrive at the ER. In either of these two intracellular schemes, it is presumed that the interchain disulphide that links A and B protomer must be cleaved before the translocation of A protomer into the cytosol (Figure 1). While the mechanism of disulfide reduction-dependent translocation is not fully understood, and may be toxin-specific, there are several evidences that cellular redox factors play essential roles in toxin translocation. My project has been focused on the important human pathogens that are A-B toxins: diphtheria toxin, tetanus and botulinum neurotoxins the etiologic agents of diphtheria, tetanus and botulism, respectively.
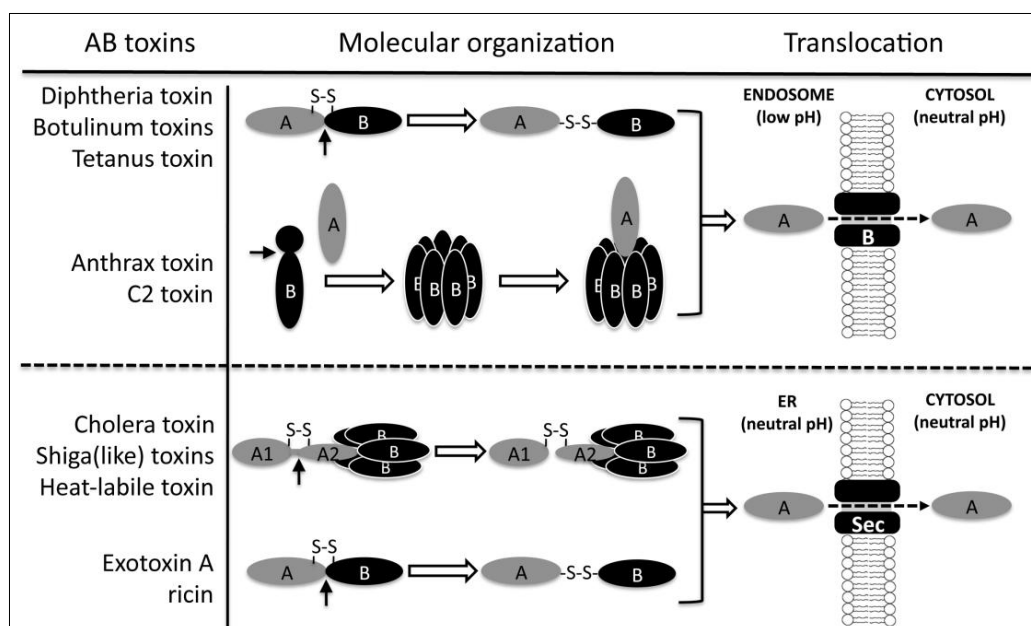

Fig. 1: Molecular organization and translocation of A-B toxins. Based on molecular organization and sites of membrane translocation, A-B toxins are divided into four groups. Group 1: the toxins are produced as a single polypeptide chain. Activation required proteolytic cleavage to generate two single polypeptide chains linked together by a disulfide bridge. Group 2: the protomers A and B are produced as separates proteins. The B protomer is activated by proteolytic cleavage and assembles into a heptameric complex that recruits the A protomer. There is no disulfide bridge. Group 3: the proteolytic cleavage occurs in the A protomer, resulting in two fragments, A1 and A2 that are linked by a disulphide bridge. Group 4: the toxins share a similar structure organization with the toxins in Group 1, but translocation occurs in the ER (Sun, 2012).

2. Diphtheria toxin structure and mechanism of action

Many bacterial toxins enter the cells via the endosomal pathway, in response to acidification as a key step of infection (Senzel *et al.,* 1998). Diphtheria toxin (DT) is an A-B toxin released

by toxigenic strains of Corynobacterium diphtheria. DT is secreted as a single polypeptide chain of 535 residues (58 kDa), and activated by a proteolytic cleavage that is catalysed by the cellular protease furin. The resulting fragments (DT-A 21 kDa and DT-B 30 kDa) remain attached via non-covalent interactions and a single interchain S-S bridge. The first step of DT cell intoxication is binding to a cell surface receptor mediated by the C-terminal domain of DT-B (Collier, 2001; Murphy, 2011). Binding triggers the endocytosis of DT inside endosomes, which become rapidly acidic following the operation of a vacuolar- type ATPase proton pump (Houtari *et al.,* 2011). The low pH triggers a structural change in DT that leads to the delivery of DT-A into the cytosol assisted by DT-B which inserts into the membrane forming a trans-membrane ion channel (Oh *et al.,* 1999). Cytosolic chaperons assist the refolding of DT-A on the cytosolic side of endosomal membrane. DT-A is then released in the cytosol upon reduction of the interchain disulphide bridge, which is the rate-limiting step of the entire process of cell entry. In the cytosol, DT-A catalyses the transfer of ADP-ribose from NAD to the elongation factor 2, causing its inactivation and the ensuing blockade of protein synthesis and cell death (Murphy, 2011). The protein monomer consists of three domains, organized to form a Y-shaped structure: i) the catalytic or C domain at the N-terminus, corresponding to fragment A, characterized by an α + β fold, ii) a β-barrel jelly-roll-like receptor or R domain at the C-terminus, and iii) a central α-helical domain, called T domain which is the portion of DT-B that inserts into the lipid bilayer upon acidification, and assists the delivery of the catalytic domain into the cytosol (Sandvig *et al.,* 1980; Collier, 2001). The exact molecular mechanism of membrane translocation mediated by the T domain is not well understood, but it is clear that the central issue is a membrane mediated refolding process. The structure of soluble T-domain at neutral pH is known, but little structural information is available for membrane-associated protein.

3. Clostridial neurotoxins

Tetanus (TeNT) and Botulinum neurotoxins (BoNTs) are A-B toxins that cause tetanus and botulism, respectively. Nine neurotoxins endowed with a metalloprotease activity have been characterized so far and are produced by neurotoxigenic anaerobic spore forming bacteria Clostridium: tetanus neurotoxin from *Clostridium tetani* and eight distinct serotypes of botulinum neurotoxins (BoNT/A to H) produced by strains or *Clostridium botulinum* or *Clostridium barati* and *Clostridium butirycum* (Schiavo *et al.,* 2000). They are the most potent tox-

ins yet known, with an estimated lethal dose for humans around 1 ng/Kg of body weight (Gill, 1982). Both neurotoxins are characterized by a remarkable neurospecificity and their catalytic cleavage at low concentrations of neuronal substrates. The main difference between these toxins is in the intensity and duration of muscle paralysis. Tetanus is characterized by violent and spasms of the head, trunk and limb muscle, resulting in spastic paralysis. Indeed, botulism is characterized by flaccid paralysis of both skeletal and autonomic nerve terminals (Johnson, 1999).

3.1 Tetanus neurotoxin

The infectious nature of tetanus toxin have been known since the very beginning of medical literature. It was Hippocrates (year 358) who described the symptoms of a paralysed patient with hypercontracted skeletal muscle (Major, 1945). He termed such a spastic paralysis tetanus, that in greek means contraction. Often, tetanus is fatal. Death follows body exhaustion and occurs by respiratory or heart failure. Tetanus still takes hundreds of thousands of lives per year, and is major cause of neonatal death in nonvaccinated areas. The bacterium *Clostridium tetani* is strictly anaerobic, it does not possess the redox enzymes necessary to reduce oxygen. The presence of the bacteria does not cause the disease but instead the toxins it produces cause the disease state. It is widespread in nature in forms of spores, that germinate under appropriate condition of very low oxygen, slight acidity and availability of nutrients (Popoff, 1995). Such conditions are present in anaerobic wounds and skin ruptures where spores can germinate, produce a protein toxin in the bacterial cytosol that is released by autolysis. *C. tetani* produces two toxins; tetanospasmin and tetanolysin. Tetanolysin is a cytolysin that increases the permeability of cellular membranes through cell lysis (Hatheway, 1995). Tetanospasmin is the cause of tetanus and is sometimes referred to as tetanus neurotoxin (TeNT), as it acts on the central nervous system. The toxin binds specifically to peripheral motoneuron nerve terminals at the neuromuscular junction (NMJ) and enters inside as yet uncharacterized vesicles. It is retroaxonally drived and discharged into the intersynaptic space formed with the inhibitory neurons of the spinal cord, which ensure the balance contraction of opposing skeletal muscle. Tetanus neurotoxin then binds to presynaptic receptors of these neurons and is endocytosed inside synaptic vesicles wherefrom the A protomer enters the cytosol thanks to the B protomer, which, at low pH forms a transmembrane protein-conducting channel. Once inside the cytosol, the tetanus A

protomer displays its metalloproteolytic activity, that is specific for the integral protein of the synaptic vesicles membrane termed VAMP (vesicle-associated membrane protein). VAMP is cleaved and can no more form a complex (the SNARE complex) with SNAP-25 and syntaxin proteins of the cytosol face of the presynaptic membrane. The consequence is that no neurotransmitter is released and the synapse of the inhibitory circuit is blocked, resulting in spastic paralysis (Montecucco et al., 2014).

3.2 Botulinum neurotoxins

Botulism was recognised and described much more later than tetanus. This later recognition is attributed to the much less evident symptoms to those of tetanus. In fact, botulism is characterised by a general muscle weakness, that affect ocular and throat muscles and then extends to the whole skeleton. In more severe cases, the flaccid paralysis is accompanied by impairment of respiration and of autonomic functions, and death may result from respiratory failure (Hatheway, 1995). Botulism is caused by intoxication with one of the eight distinct serotypes of BoNTs, indicated with letter from A to H, based on the fact that a serum raised against one toxin was not able to neutralise the others (Rummel, 2015). The spores of the different BoNTs germinate under different conditions, and the bacteria differ for nutrient and temperature requirements. These differences in growth conditions explain why, contrary to tetanus, botulism is very rare in wound infections. Usually, a BoNT is introduced by eating foods contaminated by spores of Clostridium botulinum, which are preserved under anaerobic conditions that favor germination, proliferation and toxin production (Hatheway, 1995). BoNTs bind to one of the several polysiaganglioside molecules, enriched in the presynaptic membrane at the NMJ and then to one protein of synaptic vesicles. BoNTs are then internalized inside the synaptic vesicles wherefrom the A protomer, a zinc metalloprotease, translocates into the cytosol assisted by B protomer, which forms a translocating channel following acidification of the synaptic vesicle lumen. The potency of botulinum neurotoxins is the result of an elaborate and efficient molecular mechanism of action, that impairs an essential physiological function: the neurotransmission at peripheral nerve terminals (Pantano et al., 2013). Once inside the cytosol the A protomer of BoNT/A/C/E cleave SNAP-25; the one of BoNT/B/D/F and G cleave VAMP; and the one of BoNT/C cleaves also syntaxin. So, the assembly of the nanomachine, that mediates fusion of synaptic vesicle membrane with release of neurotransmitter, is impaired and the synapse is paralysed

(Montecucco *et al.,* 2014). BoNTs bind and act on the peripheral cholinergic nerve terminals, causing flaccid paralysis of both skeletal and autonomic nerve terminals (Pantano *et al.,* 2013).

There are different vertebrates host of different BoNTs serotypes. BoNT/A/B, and E are those often related with human botulism, with fewer cases being caused by BoNT/F. Almost exclusively associated with botulism among birds is BoNT/C, whilst BoNT/D cause botulism in different animal species but not in humans. BoNT/E is more frequently associated with botulism of marine vertebrates and fish eating birds (Montecucco *et al.,* 2015; Rossetto *et al.,* 2014).

The main and life threating outcome arising from BoNTs action in vertebrates is the blockage of neurotransmitter release at the neuromuscular junction, which results in the impossibility of stimulating voluntary muscles and therefore a typical flaccid paralysis of botulism. In adults, botulism is generally caused by an intoxication through contaminated food with the toxin. Being that BoNTs are sensitive to proteolytic and denaturing conditions found in the stomach lumen. It is believed that to overcome this difficulty, they are produced as complexes with other nontoxic proteins, which enable a portion of BoNTs to reach the intestine undamaged. It is not an infection, since Clostridia colonization of the intestinal tract is quite difficult. This situation can happen in infants because ingested spores can germinate in the absence of competing resident microbiota (Rossetto *et al.,* 2014). In this latter case BoNTs are produced and released in the intestine for prolonged periods of time causing infant botulism (Aureli *et al.,* 1986; Koepke *et al.,* 2008). There are three other rare forms of botulism (Figure 2): wound botulism that results from tissue contamination with spores, and is mainly associated with drug users; iatrogenic botulism which is due to the inappropriate administration or abuse of the toxin for cosmetic or therapeutic purpose; inhalational botulism, that is correlated to inhalation of BoNT-containing aerosols, and mainly associated to a possible use of BoNTs as bioweapon (Arnon *et al.,* 2001). Despite the different forms, the symptoms of the disease are usually very similar. The facial and throat innervations are the first affected causing diplopia, ptosis and dysphagia. The paralysis continues and when respiratory muscles are involved, breathing is compromised and death comes through respiratory failure. However, since intoxicated nerves remain intact and do not degenerate, if mechanical ventilation is timely performed, patients survive fully recovering from the neuroparalysis, in a time window which depends on the amount of toxin poisoning nerve

terminals and on the BoNT serotype involved. The current therapy is aimed to neutralize circulating toxin using anti-BoNT serum and keep alive patients using artificial ventilation (Rossetto *et al.,* 2014).
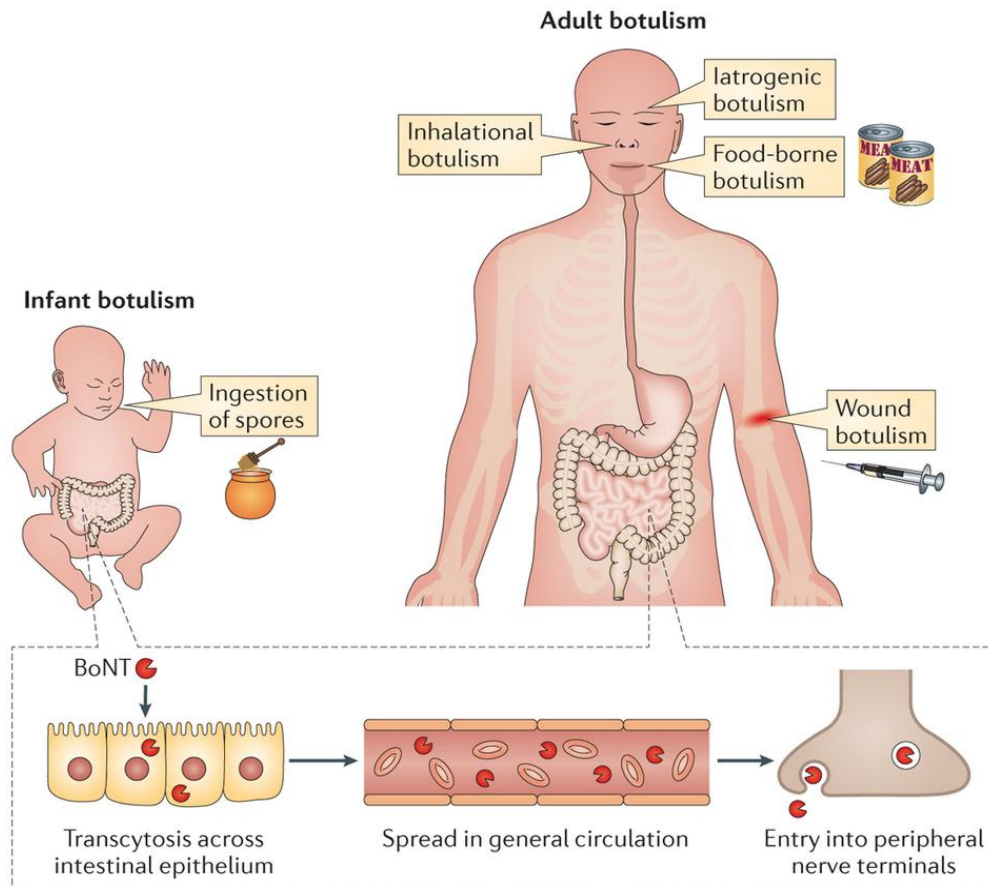

Fig. 2: Different forms of human botulism. Until now, it has been characterized five forms of human botulism. The two most common forms are food-borne botulism, that occurs following the ingestion of BoNT-containing foods, and infant botulism, that is caused by the ingestion of food contaminated with spores that germinate in the gastrointestinal tract as a consequence of the lack of a mature microbiome. The other three forms are much rarer, they include inhalational botulism, iatrogenic botulism and, wound botulism. Following transcytosis across the intestinal epithelium and entry into the general circulation, the neurotoxin enters peripheral cholinergic nerve terminals, causing the flaccid paralysis. (From Rossetto *et al.,* 2014).

4. Bacterial protein toxins in research and therapy

Bacterial toxins were the first virulence factors discovered thank to their peculiar abilities. Since their discovery, they have played an essential role both in basic and applied research and in therapy and pharmaco-cosmetics. Many essential essential cell functions were discovered thanks to the toxins that could inhibit them: this was the case in studies of trafficking (e.g. clostridial neurotoxins) and of cytoskeleton actin organisation. Also, chimera

of toxins that bind specifically to cell surface receptors and are endocytosed (e.g. diphtheria toxin) can shuttle epitopes, nucleotides or peptides into cells. This use is particularly useful in developing therapeutical approaches against cancer. Diphtheria toxin has already been utilised as anti-cancer agent. Normally the targeting is achieved by deleting the receptor binding domain, and combining the remaining portion (translocation and catalytic domain) with proteins that selectively bind to the surface of cancer cells.

Clostridial neurotoxins instead, have direct applications in therapy. BoNTs can be considered Janus toxins, as they are the most deadly exotoxins known to humans and one of the safest drugs used in several human pathologies. Indeed, considering their relative ease of production and extremely potency, BoNTs are considered by the Center for Disease Control and Prevention (CDC) as category A agents, i.e. toxins that can be used as biological weapons, but, at the same time, for their neurospecificity and reversibility, they have become very useful therapeutics for a growing and heterogeneous number of human disease characterized by peripheral nerve terminals hyperactivity (Arnon *et al.*, 2001). In addition, thanks to the comprehension of their molecular mechanism of action, BoNTs have become useful tools in the study of neuronal physiology. Botulinum neurotoxin (known as Botox) has also become a fashionable agent in cosmetic to efface wrinkles.

5. Bacterial protein toxins studied in the present thesis

During my Ph.D, I have studied the following bacterial protein toxins: diphtheria toxin, tetanus and botulinum neurotoxins from biochemical, structural and cell biology points of view. Below, I will briefly introduce the main projects I have worked. Detailed information about the toxins and the work done with them is given in the relative sections.

In part I, I include an already published article in which I studied the conformational switching of diphtheria toxin at acidic pH. DT includes within its B protomer a T domain which is known to mediate the pH-dependent membrane translocation of A, by forming a channel through which the catalytic domain cross the endocytic vesicle membrane. I reported the first crystal structure of DT obtained in the presence of lipid bicelles (which simulate the endosomal membrane) and grown at pH 5.5, pH that mimics the acidic environment where translocation takes place. The crystal structure proposed throws lights in the initial event of the membrane translocation process.

In part II, I discuss a project which aimed to unravel the three dimensional structure of tetanus neurotoxin. To develop an effective structure-based vaccine/inhibitor/antitoxin to treat tetanus victims, an understanding of the molecular mechanism at the atomic level, is a prerequisite. Though experimental three-dimensional structures are available for the N-terminal catalytic domain and C-terminal binding domain, no experimental structure is available of the entire TeNT molecule. I have performed several biochemical and structural studies to characterize the three dimensional structure of TeNT. Because TeNT is considered "uncrystallizable", I focused on the use of antibody fragments (Fabs) as crystallization chaperons to aid the structural determination. Native gel analysis and size exclusion chromatography showed the formation of a stable complex *in vitro* between TeNT and the relative Fabs. Several crystallization experiments were carried out by high throughput crystallization screens.

In part III, I show the work performed with the binding domains of several BoNT serotypes in order to study their trafficking at the neuromuscular junction. I present data of biochemical characterization of the recombinant binding domains, which are considered ideal tools for studying the initial trafficking events of BoNTs. The purified binding domains were used for *in vitro* and *in vivo* assays in order to test their functionality and their distribution along the neuromuscular junction (NMJ). The data from fluorescence analysis show high specificity of these binding domains at the NMJ, and a different staining between the several serotypes, reflecting their different time of intoxication, and perhaps a different pathway of trafficking.

5. References

1. Schiavo G, van der Goot FG. The bacterial toxin toolkit. Nat Rev Mol Cell Biol. 2001 Jul; 2(7): 530-7.

2. Kahn RA, Fu H, Roy CR. Cellular hijacking: a common strategy for microbial infection. Trends Biochem Sci. 2002 Jun; 27(6): 308-14.

3. Barth H, Aktories K, Popoff MR, Stiles BG. Binary bacterial toxins: biochemistry, biology, and applications of common Clostridium and Bacillusproteins. Microbiol Mol Biol Rev. 2004 Sep; 68(3): 373-402.

4. Jianjun Sun. Roles of celluar redox factors in pathogen and toxin entry in the endocytic pathways. Book Chapter. INTECH Open Access Publisher, 2012.

5. Senzel L, Huynh PD, Jakes KS, Collier RJ, Finkelstein A. The diphtheria toxin channel-forming T domain translocates its own NH2-terminal region across planar bilayers. J Gen Physiol. 1998 Sep; 112(3): 317-24.

6. Collier RJ. Understanding the mode of action of diphtheria toxin: a perspective on progress during the 20th century. Toxicon. 2001 Nov; 39(11): 1793-803.

7. Murphy JR. Mechanism of diphtheria toxin catalytic domain delivery to the eukaryotic cell cytosol and the cellular factors that directly participate in the process. Toxins (Basel). 2011 Mar; 3(3): 294-308.

8. Huotari J, Helenius A. Endosome maturation. EMBO J. 2011 Aug 31; 30(17) :3481-500.

9. Oh KJ, Zhan H, Cui C, Altenbach C, Hubbell WL, Collier RJ. Conformation of the diphtheria toxin T domain in membranes: a site-directed spin-labeling study ofthe TH8 helix and TL5 loop. Biochemistry. 1999 Aug 10; 38(32): 10336-43.

10. Sandvig K, Olsnes S. Diphtheria toxin entry into cells is facilitated by low pH. J Cell Biol. 1980 Dec; 87(3 Pt 1): 828-32.

11. Gill DM. Bacterial toxins: a table of lethal amounts. Microbiol Rev. 1982 Mar; 46(1): 86-94

12. Schiavo G, Matteoli M, Montecucco C. Neurotoxins affecting neuroexocytosis. Physiol Rev. 2000 Apr; 80(2): 717-66.

13. Johnson EA. Clostridial toxins as therapeutic agents: benefits of nature's most toxic proteins. Annu Rev Microbiol. 1999; 53: 551-75.

14. Major RH. Classic description of disease. Springfield, IL. 1945.

15. Popoff MR. Ecology of neurotoxigenic strains of clostridia. Curr Top Microbiol Immunol. 1995; 195: 1-29.

16. Hatheway CL. Toxigenic clostridia. Clin Microbiol Rev. 1990 Jan; 3(1): 66-98.

17. Montecucco C, and Rossetto O. Biological toxins. In: pathobiology of human disease. San Diego, Elsevier, 2014; 175-180.

18. Hatheway CL. Botulism: the present status of the disease. Curr Top Microbiol Immunol. 1995; 195: 55-75.

19. Montecucco C, Rasotto MB. On botulinum neurotoxin variability. MBio. 2015 Jan 6;6(1)

20. Pantano S, Montecucco C. The blockade of the neurotransmitter release apparatus by botulinum neurotoxins. Cell Mol Life Sci. 2014 Mar; 71(5): 793-811.

21. Rummel A. The long journey of botulinum neurotoxins into the synapse. Toxicon. 2015 Dec 1; 107(Pt A): 9-24.

22. Rossetto O, Pirazzini M, Montecucco C. Botulinum neurotoxins: genetic, structural and mechanistic insights. Nat Rev Microbiol. 2014 Aug; 12(8): 535-49.

23. Aureli P, Fenicia L, Pasolini B, Gianfranceschi M, McCroskey LM, Hatheway CL. Two cases of type E infant botulism caused by neurotoxigenic Clostridium butyricum in Italy. J Infect Dis. 1986 Aug; 154(2): 207-11.

24. Koepke R, Sobel J, Arnon SS. Global occurrence of infant botulism, 1976-2006. Pediatrics. 2008 Jul; 122(1): e73-82.

25. Centers for Disease Control and Prevention DoHaHS. Possession, use, and transfer of select agents and toxins; biennial review. Final rule. *Fed Regist.* 2012; 77(194): 61083-61115.

26. Arnon SS, Schechter R, Inglesby TV, et al. Botulinum toxin as a biological weapon: medical and public health management. *JAMA.* 2001; 285(8): 1059-1070.

27. Rossetto O, Seveso M, Caccin P, Schiavo G, Montecucco C. Tetanus and botulinum neurotoxins: turning bad guys into good by research. *Toxicon.* 2001; 39(1): 27-41.

PART I

DIPHTHERIA TOXIN CONFORMATIONAL SWITCHING AT ACIDIC pH

Diphtheria Toxin conformational switching at acidic pH

Oneda Leka, Francesca Vallese, Marco Pirazzini, Paola Berto, Cesare Montecucco, and Giuseppe Zanotti

Department of Biomedical Sciences, University of Padua, Via Ugo Bassi 58/B, 35131 Padua, Italy

Authors to whom correspondence should be addressed:

Giuseppe Zanotti, Department of Biomedical Sciences, University of Padua, Via Ugo Bassi 58/B, 35131 Padua, Italy Phone: +39 049 8276409. Fax: +39 049-8073310. Email: giuseppe.zanotti@unipd.it, URL: http://tiresia.bio.unipd.it/zanotti

Cesare Montecucco, Department of Biomedical Sciences, University of Padua, Via Ugo Bassi 58/B, 35131 Padua, Italy Phone: +39 049 8276058. Fax: +39 049-8073310. Email: cesare.montecucco@gmail.com

RUNNING TITLE: diphtheria toxin membrane interaction

ABBREVIATIONS: DT, Diphtheria Toxin; r.m.s.d., root mean square deviation; DMPC, 1, 2-dimyristoyl-sn- glycerol-3-phosphocholine; CHAPSO, 3-[(3-cholaminodopropyl) dimethylammonio]-2-hydroxy-1-propanesulfonate;

KEYWORDS: *Diphtheria toxin;* membrane translocation; bicelles; crystal structure;

Diphtheria toxin conformational switching at acidic pH

Oneda Leka, Francesca Vallese, Marco Pirazzini, Paola Berto, Cesare Montecucco and Giuseppe Zanotti

Department of Biomedical Sciences, University of Padua, Italy

Diphtheria toxin (DT), the etiological agent of the homonymous disease, like other bacterial toxins, has to undergo a dramatic structural change in order to be internalized into the cytosol, where it finally performs its function. The molecular mechanism of toxin transit across the membrane is not well known, but the available experimental evidence indicates that one of the three domains of the toxin, called the central α-helical domain, inserts into the lipid bilayer, so favoring the translocation of the catalytic domain. This process is driven by the acidic pH of the endosomal lumen. Here, we describe the crystal structure of DT grown at acidic pH in the presence of bicelles. We were unable to freeze the moment of DT insertion into the lipid bilayer, but our crystal structure indicates that the low pH causes the unfolding of the TH2, TH3 and TH4 α-helices. This event gives rise to the exposure of a hydrophobic surface that includes the TH5 and TH8 α-helices, and the loop region connecting the TH8 and TH9 α-helices. Their exposure is probably favored by the presence of lipid bilayers in the crystallization solution, and they appear to be ready to insert into the membrane.

Introduction

Diphtheria toxin (DT) is a protein toxin that causes the homonymous disease, which is currently re-emerging in those areas of the world where vaccination programs are not fully enforced [1]. DT has also been used to prepare immune-conjugates aimed at deleting selective populations of pathogenic cells [2]. DT is secreted from *Corynebacterium diphtheriae* as a unique polypeptide chain of 535 amino acids that is subsequently nicked by proteases at a loop subtended by a single disulfide bond. The resulting fragments (DT-A, 21 kDa; DT-B, 30 kDa) remain attached via noncovalent interactions and a single interchain disulfide bridge. The first step of DT cell intoxication is the binding to a cell surface receptor mediated by the C-terminal domain of DT-B [3,4]. Binding triggers the endocytosis of DT inside endosomes, which become rapidly acidic following the operation of a vacuolar-type ATPase proton pump [5]. The low pH triggers a structural change in DT that leads to the delivery of DT-A into the cytosol. This event is assisted by DT-B, which inserts into the membrane and forms a transmembrane ion channel [6]. Cytosolic chaperones assist the refolding of DT-A on

Abbreviations

C domain, catalytic domain; DMPC, dimyristoyl phosphatidylcholine; DT, diphtheria toxin; PDB, protein data bank; R domain, β-barrel jelly-roll-like receptor domain; T domain, central α-helical domain.

the cytosolic side of the endosomal membrane [4,7–9]. DT-A is then released into the cytosol upon reduction of the interchain disulfide bridge, which is the rate-limiting step of the entire process of cell entry [10]. In the cytosol, DT-A catalyzes the transfer of ADP-ribose from NAD to elongation factor 2, causing its inactivation and the ensuing blockade of protein synthesis, and eventually cell death [3].

DT is the prototype of bacterial exotoxins acting in the host cell cytosol and consisting of two disulfide-linked polypeptide chains [3,4,11,12]. Despite numerous studies, membrane translocation is the least known step of their cell intoxication mechanism [3,13]. The crystal structure of DT has been determined in monomeric and dimeric forms, with and without a nucleotide bound [14–17], and in complex with an extracellular fragment of heparin-binding epidermal growth factor [18]. However, all crystals were grown at pH 7.5. The protein monomer consists of three domains, organized to form a Y-shaped structure: (a) the catalytic domain (C domain) at the N-terminus, corresponding to fragment A, characterized by an $\alpha + \beta$-fold; (b) a β-barrel jelly-roll-like receptor domain (R domain) at the C-terminus; and (c) a central α-helical domain (T domain), which is the portion of DT-B that is supposed to insert into the lipid bilayer upon acidification, and that assists the delivery of the C domain into the cytosol [3,19,20]. It is noteworthy that the protein in the crystal can be present as a monomer or as a dimer, and a very intriguing example of domain swapping was observed in the dimeric form [21]. This dimerization was attributed to the buffer used and to a pH drop that occurred during storage of the protein at low temperature. In any case, the active form of the toxin is considered to be the monomer.

Despite the large body of indirect evidence gathered in the last 20 years on the DT-A low pH-driven membrane translocation [4,6,12,22–27], its molecular aspects remain elusive. The T domain comprises nine α-helices (Fig. 1), and it appears to have been established that the helical hairpin formed by the two strongly hydrophobic TH8 and TH9 α-helices inserts perpendicularly into the lipid bilayer. In order to allow the insertion of such helices inside the membrane, the T domain must undergo a large structural change, and there is evidence that membrane lipids do play a role in the process [12]. No structural data are available on the ion channel formed by the T domain, and nor is it known whether it is monomeric or oligomeric [28].

To obtain crystals of membrane proteins, bicelles composed of portions of lipid bilayers and detergents have been successfully introduced [29]. In an attempt to clarify the membrane translocation mechanism of
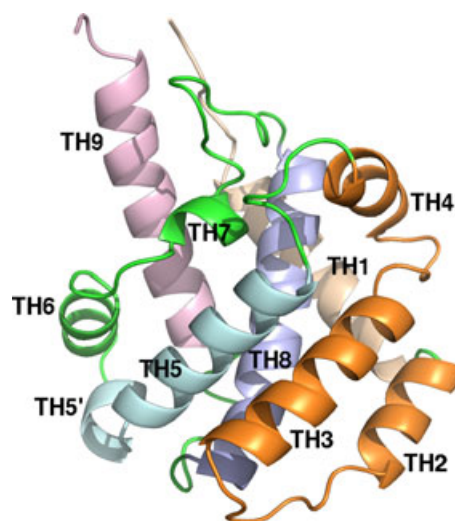

Fig. 1. Structure of the T domain of DT with α-helices labeled. Coordinates are from PDB 1MDT [15]). The three α-helices that undergo unfolding at acidic pH are colored orange; the other α-helices are shown in different colors for clarity.

DT, we have performed crystallization tests of DT at acid pH and in the presence of bicelles. At variance with other studies on the effect of pH on DT, where the isolated T domain was employed, in this work we used the entire toxin.

We report here the structure obtained at acidic pH, which reveals a relevant initial molecular event of the process.

Results and Discussion

The crystal structure of DT at acidic pH

Crystals of DT at the pH values present inside endosomes and in the presence of bicelles [dimyristoyl phosphatidylcholine (DMPC)/CHAPSO] grow as long and thin needles. They generally produce a fiber-like spectrum (Fig. S1), suggesting that the presence of bicelles and the low pH favor a conformational change of the protein structure that gives rise to a fibrous arrangement. However, in few cases and using a microfocus beam (10–20 μm), we were able to obtain a diffraction spectrum with defined Bragg peaks. The best of them resulted in a diffraction dataset at 2.8-Å resolution, but, despite the modest quality of the data obtained (Table 1), the structure could be solved by molecular replacement, and the molecular model was refined. The polypeptide chain could be traced from residues 1 to 535, with the exception of residues 188–199 and 221–266 (in chain B, from 221 to 255). The two monomers pres-

Table 1. Data collection and refinement statistics.

Wavelength (Å)	0.87290
Space group	$P2_12_12_1$
Cell dimensions	
a, b, c (Å), Z	$a = 47.44$, $b = 141.28$, $c = 176.02$, $Z = 2$
Resolution (Å)	47.44–2.80 (2.95–2.80)[a]
R_{merge}	0.192 (0.683)
R_{pim}	0.088 (0.323)
$<I/\sigma(I)>$	7.1 (2.7)
Completeness (%)	94.7 (98.2)
Multiplicity	5.5 (5.0)
Refinement	
No. of reflections	28 350
R_{work}/R_{free}	0.238/0.322
No. of protein atoms	7374
Rmsd	
Bond lengths (Å)	0.01
Bond angles (°)	1.51
Ramachandran plot (%)	
Most favored	85.3
Additionally allowed	13.5
Generously allowed	1.0
Disallowed regions	0.2
Overall G-factor	– 0.1

[a]Values in parentheses refer to the last resolution shell.

Fig. 3. Crystal structure of the monomer of DT at low pH. (A) Cartoon view of the DT monomer. The C domain is colored green, the T domain cyan, and the R domain orange. (B) Same as (A), except that the diameter of the tube is proportional to the thermal B-factor of the atoms of each residue. The most flexible parts (excluding the TH2, TH3 and TH4 α-helices, which are not visible in the structure) are the loops of the R domain; the β-sheets of this domain are quite rigid, as are all residues of the C domain. The entire T domain appears to be more flexible than the cores of the other two domains.

ent in the asymmetric unit (Fig. 2) are essentially identical (the rmsd between all Cα atoms is 0.73 Å), with the exception of a flexible region corresponding to a large portion of the TH4 α-helix (see next paragraph). The only other significant difference is represented by loop 516–522, belonging to the R domain and involved in contacts with the other monomer in the crystal. The overall folding of the DT monomer at acidic pH corresponds to that of the monomer at neutral pH [15], with its three domains, C, T, and R, organized in a Y-shaped structure (Fig. 3). At acidic pH, the entire T domain shows higher overall B-factors than the cores of the other two domains, and several loops of the R domain also appear to be quite flexible.

Comparison with DT at neutral pH

The cell parameters of our crystal are similar to those of the crystal form of the orthorhombic monomeric DT [Protein Data Bank (PDB) 1MDT [15]]. In particular, the two long cell parameters become significantly longer (141.3 Å versus 135.5 Å; 176.0 Å versus 168.5 Å), whereas the shorter one remains the same (47.4 Å versus 47.0 Å); this suggests that protonation induces some repulsion between symmetry-related molecules. In addition, the neutral pH structure crystallizes in space group $P2_12_12$, whereas our crystals belong to space group $P2_12_12_1$. A comparison between the final molecular models shows that the noncrystallographic two-fold axis that relates the two monomers present in our asymmetric unit corresponds to the

Fig. 2. (A) Cartoon view of the two monomers of DT present in the asymmetric unit. The C domain, T domain and R domain are colored green, cyan, and orange, respectively. A noncrystallographic two-fold axis runs approximately perpendicular to the plane of the paper, in the center of the image. (B) Same as (A), but showing the surface of the two molecules.
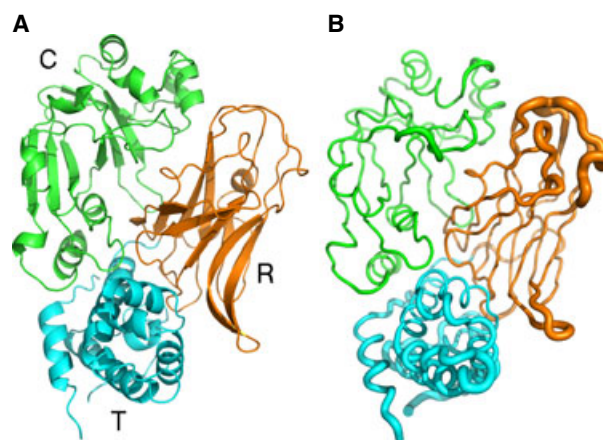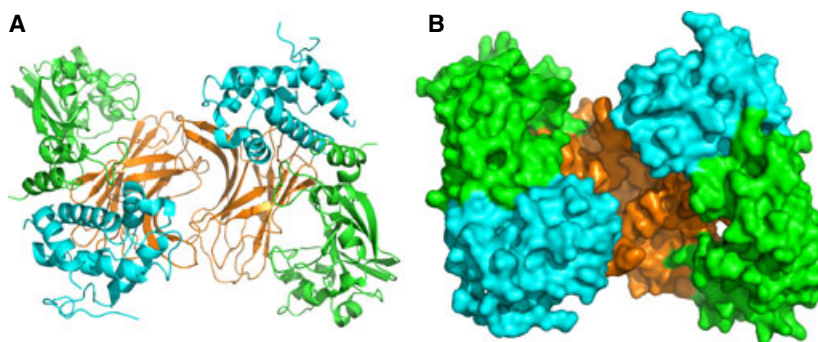
crystallographic two-fold axis of space group $P2_12_12$. In fact, molecules are packed in the crystal cell in two layers, roughly parallel, in our reference system, with the crystallographic *ac*-plane. The change of pH has no effect on the packing of the molecules in each layer, but it causes a shift of one layer with respect to the other in the *c*-direction (Fig. 4).

The structure of DT monomer at acidic pH is comparable to that at pH 7.5: the rmsd between equivalent Cα atoms is 0.90 Å for monomer A and 1.0 Å for monomer B (477 and 488 residues compared, PDB 1MDT [15]). However, a very significant difference in the structure adopted by DT at acidic pH in the presence of bicelles is the unfolding of three α-helices, TH2, TH3, and partially TH4, located at the bottom of the Y-structure of DT (in red in Fig. 5). In particular, in monomer B, the electron density for the TH2 and TH3 helices is totally absent, whereas the TH4 α-helix is partially unfolded. In monomer A, all three α-helices, TH2, TH3, and TH4, are absent, and the main chain restarts at residue 276. Other differences can be observed in the R domain, in the loop regions 407–413, 463–469, and 516–522, and from residues 494 to 507 (Fig. 5). In contrast, the structure of the catalytic domain is well preserved. Given that all available evidence indicates that unfolding of DT-A is implicated in its translocation across the lipid bilayer, our finding may suggest that the present structure represents an initial event in the process of the low pH-driven membrane insertion of DT.

Mechanisms of the conformational switch

Different mechanisms have been proposed for the conformational switching of DT triggered by acidic pH. They emerged from experiments generally performed with the isolated T domain and in the presence of lipid
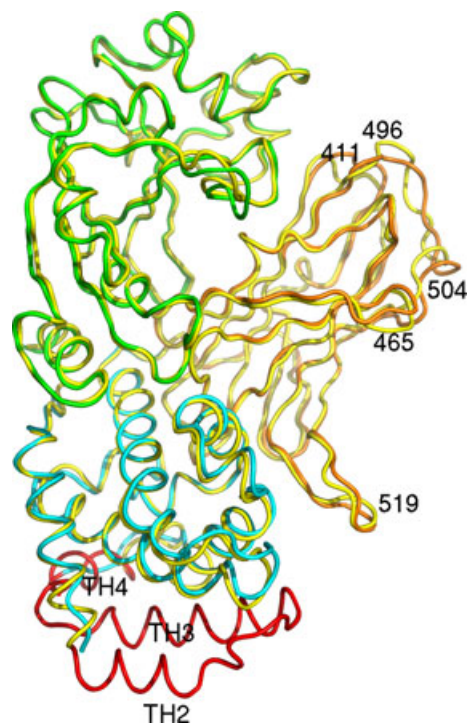

Fig. 5. Superposition of the Cα chain trace of the DT monomer at neutral and low pH. The C domain, R domain and T domain of DT at low pH are colored green, cyan, and orange, respectively, and the structure at neutral pH (PDB 1MDT) is colored yellow, with the exception of the TH2, TH3 and TH4 α-helices, which are colored red.

bilayers. Scanning mutagenesis and nitroxide derivatization experiments indicated that the TH8 α-helix and loop TL5 can insert into the bilayer [6], whereas heavy chemical modifications with a hexahistidine tag and biotin indicate the presence in the bilayer of three membrane-spanning segments, TH5, TH8, and TH9
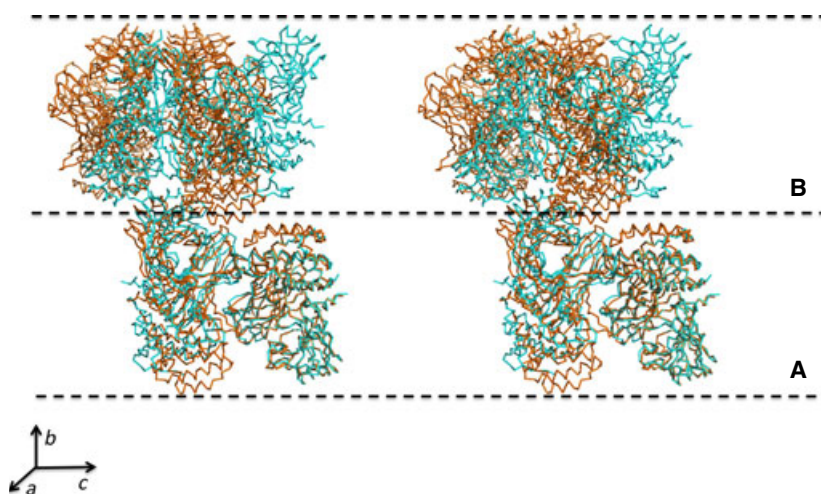

Fig. 4. Stereo view of the packing superposition of DT at acidic pH (cyan) and at neutral pH (orange). Molecules are packed in the cell in two layers, labeled A and B (the reference system is that of our crystal cell, so that the *b*-axis and the *c*-axis run in the plane of the paper in the vertical and horizontal directions, respectively). In layer A, only the two molecules present in the asymmetric unit are shown. When the molecules of the $P2_12_12$ space group [15] are superposed on layer A, molecules of layer B are shifted along the *c*-direction.

[22]. With a similar approach of chemical biotinylation of mutated residues, the TH5, TH6, TH7, TH8 and TH9 α-helices were found to be inserted into the membrane [23], and this model is also supported by fluorescence quenching experiments [26]. Experiments using the hydrophobic photoactivable reagent diamonofluorescein showed the TH1, TH8 and TH9 α-helices to be inserted into the hydrophobic core of the lipid bilayer [24]. A more comprehensive approach combining fluorescence spectroscopy with extensive molecular dynamics [30] suggests that the first step of the conformational transition is represented by the partial loss of the TH1 and TH2 helical structure, an event that allows the exposure of the hairpin formed by the TH8 and TH9 α-helices and their access to the membrane. At variance with this, the present structure indicates that the first portion of the T domain to unfold comprises the TH2, TH3 and partially the TH4 α-helices (Fig. 5). The present work is in agreement with the recent indication that a key event in the destabilization of the conformation of the T domain is the protonation of two histidines: His257 located at the end of the TH3 α-helix, and His223, located in the loop connecting the TH1 and TH2 α-helices [27, 37]. This loop was suggested to act as a safety latch, by modulating the protonation of His257 and preventing premature unfolding [12]. The side chains of the two histidines face each other, and their protonation is likely to induce a repulsion that destabilizes the TH2–TH3 hairpin, thus causing the disordering of both helices. The disordered area is heavily charged, as it contains seven lysines and nine glutamates, but they are probably unaffected at pH 6.

The unfolding of the TH2, TH3 and TH4 α-helices exposes a hydrophobic surface (Fig. 6), which includes the TH5 and TH8 α-helices and the loop region connecting the TH8 and TH9 α-helices. The latter area, in fact, shows some differences from the structure of DT at neutral pH. It must be stressed that our crystals were grown

in the presence of bicelles and, notably, the same crystals were not obtained without bicelles at the same pH value. Despite the fact that crystals did not grow inside the bicelles, it is reasonable to consider that the presence of lipids stabilizes the hydrophobic surface generated by the unfolding of the TH2, TH3 and TH4 α-helices. It is therefore safe to speculate that our structure may well represent the first molecular event in the low pH-driven process of the membrane insertion of DT-B.

Conclusions

The present article describes the first structure of the entire DT molecule grown in the presence of lipidic bicelles that mimic the membrane. It sheds light on the first molecular events in the complex process of membrane insertion of DT, with translocation of its C domain. In fact, it indicates that the first part of the molecule to change structure following protonation includes the TH2 and TH3 α-helices at the bottom of the molecule, which would uncover a hydrophobic region, and the TH4 α-helix, which is located in a region critical for the interaction between the T domain and the receptor-binding domain. This region includes several high-pK_a carboxylate residues involved in the formation of salt bridges with a group of cationic residues.

Experimental procedures

Crystallization

DT was purified and nicked as described previously [10]. The toxin was dialyzed overnight against 50 mM NaCl and 100 mM $Na_3C_6H_5O_7$ (pH 7.2), and its final concentration was adjusted to 5 mg·mL^{-1}. Bicelles were prepared by mixing appropriate amounts of DMPC and CHAPSO to reach a DMPC/CHAPSO molar ratio of 2.8 : 1. After the components had been mixed, an aqueous solution was added in
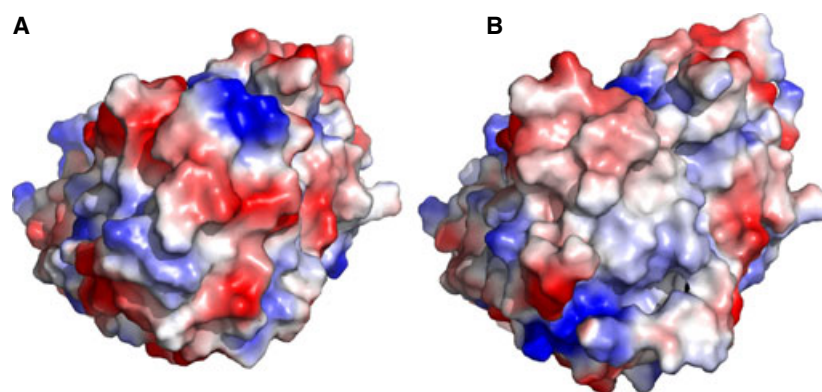
A   **B**

Fig. 6. Qualitative electrostatic potential surface of the entire DT monomer at neutral pH (A) and of the DT monomer at low pH (B). The view is rotated, with respect to Fig. 5, by ~ 90° along a horizontal axis. In (A), the hydrophilic surface is mainly formed by the TH2 and TH3 α-helices, whereas the hydrophobic portion exposed in (B) is mostly formed by the TH5 and TH8 α-helices.
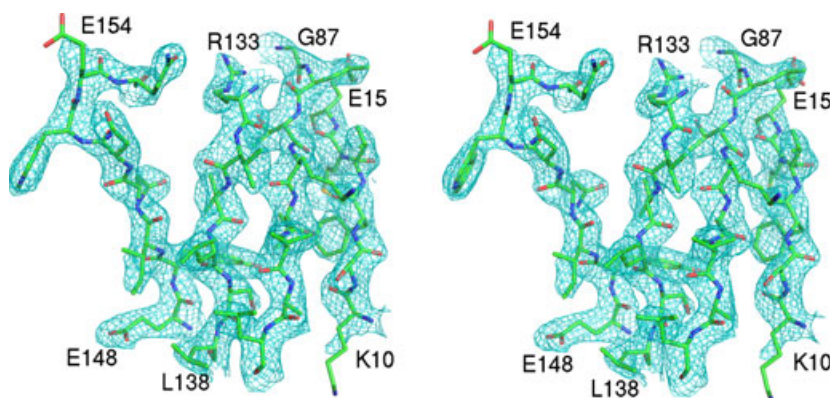
Fig. 7. Stereo view of a portion of the electron density map. The map was calculated with coefficients $2F_{obs} - F_{calc}$, and contoured at 1.5σ. A region of a β-sheet of the C domain is shown.

order to reach a total lipid concentration of 40% (w/v). Bicellar suspensions were prepared by several cycles of ultrasonic dispersion at 52 °C in a bath-type sonicator (Falc Instruments, Treviglio, Italy), and freezing until the samples became transparent. Bicelles were then mixed with the protein at a protein/bicelle ration of 4 : 1 (v/v). The pH of the DT/bicelle mixture was lowered by dialysis at room temperature, with a Slide-A-Lyser dialysis cassette (Fermentas, Thermo Fischer Scientific, Vilnius, Lithuania), with a 2-kDa cut-off, and 2 M HCl being added to the medium drop by drop until a pH of 5, 6.0 or 6.5 was achieved. These pH values were chosen because they are estimated to be present in the endosomal lumen or close to the luminal surface of the endosomal membrane. Crystals were obtained at 20 °C with the hanging drop method by mixing 2 μL of the protein/bicelle mixture with 1 μL or 2 μL of precipitant solution containing 0.1 M sodium chloride, 0.1 M magnesium chloride, 0.1 M Hepes (pH 8) and 11% w/v poly(ethylene glycol) 1500 (solution C9 MemGold HT-96; Molecular Dimensions Ltd., Newmarket, Suffolk, UK) or 0.2 M magnesium chloride, 0.1 M Tris/HCl (pH 8.5), and 25% w/v poly(ethylene glycol) 4000 (solution E6).

Structure determination and refinement

A large number of crystals, > 45, were mounted and tested at the ID23-2 microfocus beamline of the European Synchrotron Radiation Facility (Grenoble, France) or at the PXII beamline of the Synchrotron Light Source of the PSI facility in Villigen (Zurich, Switzerland). They generally showed a fiber-like diffraction spectrum, with axial reflections corresponding to a repetition period of ~ 43 Å. The use of only a few crystals gave rise to a spectrum with Bragg peaks in some orientations, and in a few cases it was possible to obtain a complete diffraction dataset. The best native dataset, diffracting at 2.8-Å maximum resolution, was measured from a crystal grown from solution E6. The final pH of the drop in this condition was 6. Data were indexed and integrated with XDS [31] and merged and scaled with SCALA [32]. Crystals belong to the orthorhombic space

group P2₁2₁2₁, with the following unit cell dimensions: a = 44.74 Å, b = 141.28 Å, and c = 176.02 Å. Two monomers are present in the asymmetric unit, corresponding to a V_M of 2.45 Å³/Da and an approximate solvent content of 50%. The structure was solved by molecular replacement with the structure of monomeric DT (PDB 1MDT [15]) as the template, by use of MOLREP contained in the CCP4 crystallographic package [33]. The model was manually adjusted with COOT [34]. Refinement was carried with PHENIX [35]. The final crystallographic *R*-factor is 0.238 (R_{free} = 0.322). Owing to the low resolution, no solvent molecules were added. The relatively high *R*-factor is justified by the very small crystal sizes and their low diffraction power, as also indicated by the high R_{merge} value. The electron density map is quite good (Fig. 7). Geometrical parameters of the models, checked with PROCHECK [36], are generally better than expected for this resolution. Data collection and refinement statistics are summarized in Table 1.

Acknowledgements

Author contributions

C. Montecucco and G. Zanotti planned the experiments. O. Leka, F. Vallese and P. Berto performed crystallization tests. O. Leka, F. Vallese and M. Pirazzini measured diffraction data. G. Zanotti processed data and refined the crystal structure. G. Zanotti and C. Montecucco, along with all other authors, contributed to the writing of the paper.

References

1 Galazka A (2000) Implications of the diphtheria epidemic in the Former Soviet Union for programs. *J Infect Dis* **181** (Suppl 1), S244–S248.

2 Kreitman RJ (2009) Recombinant immunotoxins containing truncated bacterial toxins for the treatment of hematologic malignancies. *BioDrugs* **23**, 1–13.

3 Collier RJ (2001) Understanding the mode of action of diphtheria toxin: a perspective on progress during the 20th century. *Toxicon* **39**, 1793–1803.

4 Murphy JR (2011) Mechanism of diphtheria toxin catalytic domain delivery to the eukaryotic cell cytosol and the cellular factors that directly participate in the process. *Toxins (Basel)* **3**, 294–308.

5 Huotari J & Helenius A (2011) Endosome maturation. *EMBO J* **30**, 3481–3500.

6 Oh KJ, Zhan H, Cui C, Altenbach C, Hubbell WL & Collier RJ (1999) Conformation of the diphtheria toxin T domain in membranes: a site-directed spin-labeling study of the TH8 helix and TL5 loop. *Biochemistry* **38**, 10336–10343.

7 Ratts R, Zeng HY, Berg EA, Blue C, McComb ME, Costello CE, VanderSpek JC & Murphy JR (2003) The cytosolic entry of diphtheria toxin catalytic domain requires a host-cell cytosolic translocation factor complex. *J Cell Biol* **160**, 1139–1150.

8 Lemichez E, Bomsel M, Devilliers G, vanderSpek J, Murphy JR, Lukianov EV, Olsnes S & Boquet P (1997) Membrane translocation of diphtheria toxin fragment A exploits early to late endosome trafficking machinery. *Mol Microbiol* **23**, 445–457.

9 Chassaing A, Pichard S, Araye-Guet A, Barbier J, Forge V & Gillet D (2011) Solution and membrane-bound chaperone activity of the diphtheria toxin translocation domain towards the catalytic domain. *FEBS J* **278**, 4516–4525.

10 Papini E, Rappuoli R, Murgia M & Montecucco C (1993) Cell penetration of diphtheria toxin. Reduction of the interchain disulfide bridge is the rate-limiting step of translocation in the cytosol. *J Biol Chem* **268**, 1567–1574.

11 Montecucco C, Papini E & Schiavo G (1994) Bacterial protein toxins penetrate cells via a four-step mechanism. *FEBS Lett* **346**, 92–98.

12 Ladokhin AS (2013) pH-triggered conformational switching along the membrane insertion pathway of the diphtheria toxin T-domain. *Toxins (Basel)* **5**, 1362–1380.

13 Wu Z, Jakes KS, Samelson-Jones BS, Lai B, Zhao G, London E & Finkelstein A (2006) Protein translocation by bacterial toxin channels: a comparison of diphtheria toxin and colicin Ia. *Biophys J* **91**, 3249–3256.

14 Choe S, Bennett MJ, Fujii G, Curmi PM, Kantardjieff KA, Collier RJ & Eisenberg D (1992) The crystal structure of diphtheria toxin. *Nature* **357**, 216–222.

15 Bennett MJ & Eisenberg D (1994) Refined structure of monomeric diphtheria toxin at 2.3 A resolution. *Protein Sci* **3**, 1464–1475.

16 Bell CE & Eisenberg D (1996) Crystal structure of diphtheria toxin bound to nicotinamide adenine dinucleotide. *Biochemistry* **35**, 1137–1149.

17 Bell CE & Eisenberg D (1997) Crystal structure of diphtheria toxin bound to nicotinamide adenine dinucleotide. *Adv Exp Med Biol* **419**, 35–43.

18 Louie GV, Yang W, Bowman ME & Choe S (1997) Crystal structure of the complex of diphtheria toxin with an extracellular fragment of its receptor. *Mol Cell* **1**, 67–78.

19 Draper RK & Simon MI (1980) The entry of diphtheria toxin into the mammalian cell cytoplasm: evidence for lysosomal involvement. *J Cell Biol* **87**, 849–854.

20 Sandvig K & Olsnes S (1980) Diphtheria toxin entry into cells is facilitated by low pH. *J Cell Biol* **87**, 828–832.

21 Bennett MJ, Choe S & Eisenberg D (1994) Domain swapping: entangling alliances between proteins. *Proc Natl Acad Sci USA* **91**, 3127–3131.

22 Senzel L, Gordon M, Blaustein RO, Oh KJ, Collier RJ & Finkelstein A (2000) Topography of diphtheria toxin's T domain in the open channel state. *J Gen Physiol* **115**, 421–434.

23 Rosconi MP, Zhao G & London E (2004) Analyzing topography of membrane-inserted diphtheria toxin T domain using BODIPY-streptavidin: at low pH, helices 8 and 9 form a transmembrane hairpin but helices 5–7 form stable nonclassical inserted segments on the cis side of the bilayer. *Biochemistry* **43**, 9127–9139.

24 D'Silva PR & Lala AK (2000) Organization of diphtheria toxin in membranes. A hydrophobic photolabeling study. *J Biol Chem* **275**, 11771–11777.

25 Chenal A, Prongidi-Fix L, Perier A, Aisenbrey C, Vernier G, Lambotte S, Haertlein M, Dauvergne M-T, Fragneto G, Bechinger B *et al.* (2009) Deciphering membrane insertion of the diphtheria toxin T domain by specular neutron reflectometry and solid-state NMR spectroscopy. *J Mol Biol* **391**, 872–883.

26 Wang J & London E (2009) The membrane topography of the diphtheria toxin T domain linked to the a chain reveals a transient transmembrane hairpin and potential translocation mechanisms. *Biochemistry* **48**, 10446–10456.

27 Rodnin MV, Kyrychenko A, Kienker P, Sharma O, Posokhov YO, Collier RJ, Finkelstein A & Ladokhin AS (2010) Conformational switching of the diphtheria toxin T domain. *J Mol Biol* **402**, 1–7.

28 Gordon M & Finkelstein A (2001) The number of subunits comprising the channel formed by the T domain of diphtheria toxin. *J Gen Physiol* **118**, 471–480.

29 Ujwal R & Bowie JU (2011) Crystallizing membrane proteins using lipidic bicelles. *Methods* **55**, 337–341.

30 Kurnikov IV, Kyrychenko A, Flores-Canales JC, Rodnin MV, Simakov N, Vargas-Uribe M, Posokhov YO, Kurnikova M & Ladokhin AS (2013) pH-triggered conformational switching of the diphtheria toxin T-domain: the roles of N-terminal histidines. *J Mol Biol* **425**, 2752–2764.

31 Kabsch W (2010) Integration, scaling, space-group assignment and post-refinement. *Acta Crystallogr D Biol Crystallogr* **66**, 133–144.

32 Evans P (2006) Scaling and assessment of data quality. *Acta Crystallogr D Biol Crystallogr* **62**, 72–82.

33 Winn MD, Ballard CC, Cowtan KD, Dodson EJ, Emsley P, Evans PR, Keegan RM, Krissinel EB, Leslie AGW, McCoy A *et al.* (2011) Overview of the CCP4 suite and current developments. *Acta Crystallogr D Biol Crystallogr* **67**, 235–242.

34 Emsley P, Lohkamp B, Scott WG & Cowtan K (2010) Features and development of Coot. *Acta Crystallogr D Biol Crystallogr* **66**, 486–501.

35 Adams PD, Afonine PV, Bunkóczi G, Chen VB, Davis IW, Echols N, Headd JJ, Hung L-W, Kapral GJ,

Grosse-Kunstleve RW *et al.* (2010) PHENIX: a comprehensive Python-based system for macromolecular structure solution. *Acta Crystallogr D Biol Crystallogr* **66**, 213–221.

36 Laskowski RA, Rullmannn JA, MacArthur MW, Kaptein R & Thornton JM (1996) AQUA and PROCHECK-NMR: programs for checking the quality of protein structures solved by NMR. *J Biomol NMR* **8**, 477–486.

37 Perier A, Chassaing A, Raffestin S, Pichard A, Masella M, Ménez A, Forge V, Chenal A & Gillet D (2007) Concerted protonation of key histidines triggers membrane interaction of the diphtheria toxin T domain. *J. Biol. Chem.* **282**, 24239–24245.

Supporting information

Additional supporting information may be found in the online version of this article at the publisher's web site:

Fig. S1. Central view of diffraction images of two different fiber-like crystals of DT.

PART II

STRUCTURAL CHARACTERIZATION OF TETANUS NEUROTOXIN USING

ANTIBODY FRAGMENTS AS TOOLS FOR THE CRYSTALLIZATION

PART II: STRUCTURAL CHARACTERIZATION OF TETANUS NEUROTOXIN USING ANTIBODY FRAGMENTS AS TOOLS FOR THE CRYSTALLIZATION

1. INTRODUCTION

1.1 Molecular structure and properties of tetanus neurotoxin

Tetanus neurotoxin (TeNT) acts on the central nervous system by inhibiting neurotransmitter release and causing spastic paralysis. TeNT binds to peripheral neuronal synapses, is internalized and moves by retrograde transport up the axon into the spinal cord where it can move between postsynaptic and presynaptic neurons. It is produced by Clostridium tetani but shares 65 % sequence homology and 35% identity with BoNT serotypes. TeNT is a single polypeptide of 1315 aminoacids residues, approximately of 150 kDa. The toxin is composed of a heavy chain (HC) and a light chain (LC) linked together by a disulphide bond. The binding and the translocation domains are located in the heavy chain, whereas the catalytic domain resides in the light chain of the molecule (Johnson, 1999; Pellizari *et al.,* 1999). It is a zinc metalloproteases, Zn^{2+} dependent, and heavy-metal chelators generate inactive apo-neurotoxin. TeNT cleaves VAMP, at an identical site cleaved by BoNT/B (Schiavo *et al.,* 1992; Schiavo *et al.,* 1992; Lalli *et al.,* 1999).
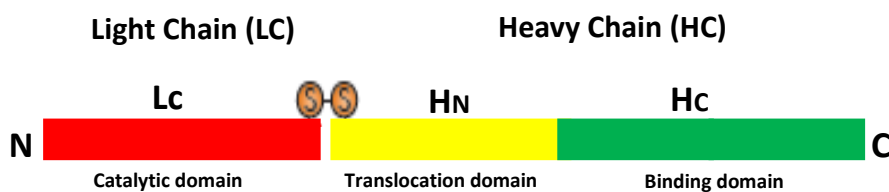

Fig. 2.1: Domain organization of Tetanus neurotoxin. Every of that encompasses a specific role in cell mechanism of intoxication: the Hc domain binds specifically to nerve terminals; the H_N domain translocate the L chain into the nerve terminal cytosol; and L chain is a metalloprotease that cleaves and inactivates specific SNARE proteins that are involved in neurotransmitter release, thereby causing neuroparalysis (Adapted from Pellizari *et al.,* 1999).

The two chains, based on their functionality properties, can be divided into three domains (Fig. 2.1): (I) Hc (50 kDa, in green) is involved in nerve terminal binding and internalization; (ii) H_N (50 kDa, in yellow), assists the translocation of the catalytic part of the toxin from the

internal part of mature endosomes into the neuronal cytosol; (iii) the Lc, catalytic domain (50 kDa, in red) is a metalloprotease that cleaves the SNARE proteins interfering with the release of neurotransmitters that results in a reversible neuroparalysis. Despite the amino acid sequence variability among the Clostridial neurotoxins variants, the structure organization is however maintained, as it mechanism of nerve intoxication (Schiavo *et al.,* 1992).

The early step in tetanus toxin internalization is cell binding, that is mediated by the receptor binding domain (Hc). The structure of the recombinant 50 kDa Hc has been solved by X-ray crystallography and it showed that it was structurally similar to the BoNTs binding domain (Emsley *et al.,* 2000; Fotinou *et al.,* 2001). It is organised in two subdomains: an amino-terminal lectin-like jelly-roll subdomain (H_{CN}, residues 865- 1110) and a carboxyl-terminal beta-trefoil subdomain ($H_{CC,}$ residues 1110-1315) linked by a single chain. Each of these subdomains is composed of beta-sheets joined by loops that protrude from the molecule (Fig. 2.2, A). In particular, the beta-trefoil subdomain (H_{CC}) seems to have a relevant role in ganglioside binding than does the amino-terminal lectin like subdomain, which was demonstrated by analyzing the localization of these binding domain. Instead, it is still unclear that what role plays the H_{CN} domain during intoxication. Several hypothesis suggest a function as a rigid, complex spacer between H_N and H_{CC}- domain as well as an involvement in the translocation process (Brunger and Rummel, 2009).

Gangliosides are in the category of glycosphingolipids that are found predominately in neuronal tissues. They consist of sialic acid linked to a sugar (glucose, galactose, GalNAc, GlcNAc and/or fructose) backbone attached to a ceramide base. Gangliosides make up approximately 10% of a neuron's total lipid content and they have function in cell signal transduction. Hc of tetanus toxin preferentially binds to the gangliosides, in particular the GT1b (Mocchinetti, 2005). A synthetic analogue of the GT1-b ganglioside was made in order to increase solubility because a crystal structure of the Hc and native GT1-b could not be obtained (Fotinou *et al.,* 2001). Through binding studies it was also shown that the aminoacid residues tryptophan 1288, histidine 1270 and aspartate 1221 are critical for the binding of Hc to ganglioside GT1b (Louch *et al.,* 2002). Although the affinity of Hc for gangliosides has been widely characterized, another hypothesis suggest that a high affinity receptor is involved in TeNT binding and internalization. Schiavo and co-workers proposed and demonstrated that a 15 kDa surface glycoprotein interacts with tetanus toxin in neuronal cell lines and motor neuron (Bercsenyi *et al.,* 2014). The same group has also suggested that a GPI anchored

protein Thy-1 can interact with tetanus toxin to mimic ganglioside binding (Herreros *et al.,* 2001). In addition, After internalization into the motor neuron membrane TeNT is transported via retrograde axonal transport and so reach the central nervous system.
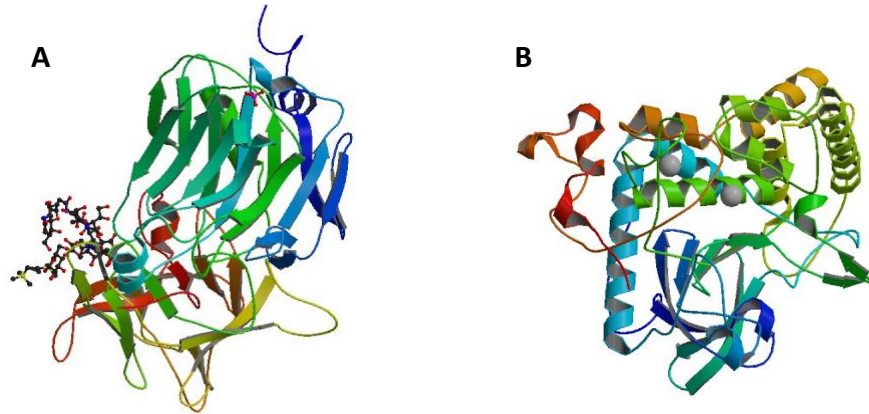

Fig. 2.2: Crystal structures of Hc-TeNT and Lc-TeNT. (A) Crystal structure of TeNT binding domain complexed with a synthetic GT1b analogue, PDB 1FV2. (B) Crystal structure of TeNT light chain, PDB 1Z7H.

After cell binding and internalisation into neuronal cells, the toxin is translocated from mature endosomes into neuronal cytoplasm. TeNT can form channels in lipid membranes when a structural change in its translocation domain is induced by the acidification of the endosomal environment (Sheridan, 1998). The translocation domain fold is markedly different from the folds observed in other toxins that undergo pore formation and translocation (Lacy and Stevens, 1998). It occludes access to a large, negatively charged cleft leading into the active-site zinc ion of the catalytic domain. The translocation domain is able to form channel in artificial bilayers (Blaustein *et al.,* 1987) visualized through electron cryomicroscopy. A requisition for the channel formation seems to be the oligomerization of four the amphipathic alpha-helices of the translocation domain. But, to date there is no molecular mechanism, by which pH triggers the translocation domain to change structure and form a membrane-spanning channel.

Experimental three-dimensional structure is available also for the N-terminal catalytic domain of tetanus toxin (Breidenbach MA and Brunger, 2005; Rao *et al.,* 2005; Fig. 2.2, B). The overall structure of TeNT-LC is similar to the other known CNT light chain structures. Differences between TeNT-LC and the other CNT light chains are mainly limited to surface features such as unique electrostatic potential profiles. The catalytic domain shares 51,6% sequence identity with Botulinum neurotoxin type B. It contains the HEXXH motif, typical of many zinc proteases. Other than this motif, the catalytic domain shares no sequence

similarity with proteins outside the Clostridial family. The TeNT-Lc crystallographic structure shows the active site located deep inside a cavity by which the substrate gains access to the active site. The active site is centered around a zinc cation directly coordinated by residues His232, His 236 and Glu270 (Rao *et al.,* 2005).

Considering that several complete crystallographic structures of BoNTs (BoNT/A, Lacy *et al.,* 1998; BoNT/B, Swaminathan *et al.,* 2000; BoNT/E, Kumaran *et al.,* 2009) are available, there is no complete crystallographic structure for TeNT, although the high sequence similarity, the same domain organization and mechanism of action, between the above Clostridial neurotoxins. Unraveling the three dimensional structure of TeNT could provide valuable information about the molecular mechanism of membrane translocation, a step which is still unclear not only for TeNT but also for all the BoNT serotypes. TeNT is also among the most poisonous substances on Earth and major cause of neonatal death in non-vaccinated areas. Chemically modified TeNT with formaldehyde, is the most used human vaccine. However, it is believed that genetically modified toxin better preserve immunogenicity than chemical modification. To develop an effective structure-based vaccine/inhibitor/antitoxin to treat tetanus victims, an understanding of the molecular mechanism at the atomic level, is a prerequisite. So the aim of this project was the structural investigation of TeNT through crystallization studies. Because TeNT is considered "uncrystallizable" I focused on the use of antibody fragments (Fabs) as crystallization chaperons to aid the structural determination. I determined the in vitro conditions for a complex formation between TeNT and the respective Fabs screened. I could obtain binary and ternary complexes, that were analysed in vitro for stability and solubity, and *in vivo* tested for their protection ability against tetanus infection. The whole work was carried out in collaboration with Prof. Antonio Lanzavecchia at IBR, Bellinzona, Switzerland; and with Prof. Giuseppe Zanotti at the Department of Biomedical Sciences, University of Padova, Italy.

2. MATERIAL AND METHODS

Reagents and proteins. All chemicals used were from Sigma Aldrich. TeNT was previously isolated from culture filtrates of *C.tetani* strain Y-IV-3 (WS 15), frozen in liquid nitrogen and stored at -80°C in 10 mM Hepes-Na, 50 mM sodium chloride, pH 7.2. The human monoclonal antibody and the fragments derived from these antibodies (Fabs) were kindly gifted by prof. A. Lanzavecchia, IBR, Bellinzona, Switzerland.

Determination of the binding sites of the human monoclonal antibody. Full-length TeNT and Hc-TeNT (a kindly gift of Prof. T. Binz, Hannover, Germany) were used for the determination of the binding site. 1ug of each was loaded onto 4-12% SDS-Page gel (ThermoFischer Scientific) and separated by electrophoresis in 1X MES buffer. Proteins were transfered onto Potran nitrocellulose membranes (Whatman) and saturated for 1 h in PBST (1X PBS with 0.1% Tween20). After saturation the nitrocellulose membranes were incubated with all the series of antibodies in order to identify their binding site. The membranes were then washed three times with PBST and incubated with a secondary anti human antibody-HRP conjugated. Finally, membranes were washed twice with PBST and one with PBS. Visualization was carried out using Luminata Crescendo (Merck Millipore). If both TeNT and TeNT-Hc will be visualized the binding site of the antibody is the binding domain. If will be visualized just TeNT the binding site is the translocation domain, H_N.

Cerebellar Granule Neurons (CGN) cultures. Primary cultures of rat cerebellar granule neurons (CGNs) were prepared from 6- to 8-days-old rats. Cerebella were isolated, mechanically disrupted and then trypsinized in the presence of DNase I. Cells were then plated into 24 well plates, pre-coated with poly-L-lysine (50 µg/mL), at a cell density of 4 x 105 cells per well. Cultures were maintained at 37 °C, 5% CO2, 95% humidity in BME supplemented with 10% fetal bovine serum, 25 mM KCl, 2 mM glutamine and 50 µg/mL gentamicin (indicated as complete culture medium). To arrest growth of non-neuronal cells, cytosine arabinoside (10 µM) was added to the medium 18–24 h after plating.

TeNT *in vitro* inhibition assay. TeNT was first incubated in reducing buffer (150mM NaCl, 10mM NaH_2PO_4, 15mM DTT, pH 7.4) and in the presence of different concentrations of human monoclonal antibody, for 30min at 37°C. Then, CGNs at 6-8 days *in vitro* were treated with 1 nM TeNT in complete medium and left for 3.5 hours at 37 °C. For immunoblotting analysis, cells were directly lysed with reducing Laemmli sample buffer containing protease

inhibitors (complete Mini EDTA-free, Roche). Equal amounts of protein were loaded onto a 4-12% NuPage gel. The inhibition of the proteolytic activity of TeNT was evaluated using a specific antibody against VAMP2 (Synaptic System, 104 211).

Mouse lethality assay. All experiments were performed in accordance with the European Communities Council Directive n°2010/63/UE and approved by the Italian Ministry of Health. Lethality assays were performed using Swiss-Webster adult male CD1 mice weighing 26-28g. Mice were intraperitoneally injected with 4pg/g TeNT, pre-incubated for 1h at room with the Fabs. Mice were monitored every day (for 1 week), after which the experiments was considered ended. Results are displayed as Kaplan-Meyer plots, and analysed with a Mantel-Cox test for statistical significance.

Native gel analysis and Size Exclusion Chromatography. *In vitro* reaction between TeNT and Fabs was done overnight at 4°C, stiring. The complex formed was visualized in 4-16% Native-PAGE gel (ThermoFischer, Scientific) and purified from unbound Fab by gel filtration (Superdex 200 10/30**,** GE).

Crystallization. Proteins, like many molecules, can be prompted to form crystals when placed in the appropriate conditions. In order to crystallize a protein, the purified protein undergoes slow precipitation from an aqueous solution. As a result, individual protein molecules align themselves in a repeating series of "unit cells" by adopting a consistent orientation. The importance of protein crystallization is that it serves as the basis for X-ray crystallography, wherein a crystallized protein is used to determine the protein's three-dimensional structure via X-ray diffraction. The reason X-rays are used is that their wavelength range is of the same order of magnitude as chemical bonds, thus allowing obtaining an image with a resolution equivalent to interatomic distances (0.8–2.5 Å). Two of the most commonly used methods for protein crystallization fall under the category of vapor diffusion. These are known as the **hanging drop** and **sitting drop** methods. Both entail a droplet containing purified protein, buffer, and precipitant being allowed to equilibrate with a larger reservoir containing similar buffers and precipitants in higher concentrations. Initially, the droplet of protein solution contains an insufficient concentration of precipitant for crystallization, but as water vaporizes from the drop and transfers to the reservoir, the precipitant concentration increases to a level optimal for crystallization. Since the system is in equilibrium, these optimum conditions are maintained until the crystallization is complete.

Hanging drop: the drop, containing the protein and the precipitant, is placed on a silinized coverslip (which confers to the drop a semi spherical shape for a uniform evaporation), it is then inverted and used to seal the system.

Sitting drop: the drop, containing the protein and the precipitant, is placed on a depression in a microbridge in the well. The system is sealed with an object slide or crystal clear tape.

Many different crystallization trials with TeNT-104, TeNT-110 and TeNT-104-110 complexes were performed at both 4 and 20°C. The crystal plates were done using robotic system. The crystallization kits tested are the following: Jcsg Core I-IV, PACTscreen, PEGsSuite, The Classic Suite (Qiagen), JcsgPlus, Structure screen I-II, MemGold I and II, MemGold plus (Molecular Dimensiion).

3. RESULTS AND DISCUSSION

In vitro **screening of the human monoclonal antibodies (hu-mAb).** Considering the three domain organization (Hc- binding domain; HN- translocation domain; LC-catalytic domain) of the TeNT, we first determined the binding sites of each hu-mAb. Through western blotting analysis and by using a secondary human antibody we blotted the heavy chain of TeNT (TeNT-HC, 100kDa) and the recombinant binding domain of TeNT (TeNT-Hc, 50kDa). If from the western blotting are visualized both bands of TeNT-HC and TeNT-Hc the hu-mAb binds to the binding domain of the toxin. Instead if it is visualized only the band of TeNT-HC the antibody binds to the translocation domain of the toxin.

Antibody	Concentration (ug/ml)	AB Binding Area (via WB)	Inhibitory Ability CGNs (*in vitro*)	TeNT:AB Concentration
TT4	46.2	HC	-	
TT13	8.0	—	-	
TT13.1	1.8	HC	-	
TT16	21.2	—	-	
TT33	1.8	—	-	
TT39.7	8.0	HC	+	1nM:5nM
TT102	8.1	HN	-	
TT103	48.5	HC	-	
TT104.14	0.737	HC	+	1nM:2.5nM
TT107	39.8	HC	+	1nM:100nM
TT108	40.5	HC	-	
TT109	13.4	HC	+	1nM:10nM
TT110	20.3	HN	+	1nM:0.5nM
TT114	26.9	HC	-	
TT115	3.6	HN	-	

Fig. 2.3: *In vitro* **screening of human monoclonal antibody (hu-mAb) against TeNT.** In the first column are shown the whole set of human monoclonal antibodies screened. The second column the concentration of each antibody. In the third column are shown the result from the western blotting analysis for the determination of the binding sites. In the fourth column are summarized the results from the *in vitro* inhibitory assays on CGNs. The fifth column shows the lower concentration at which the antibodies gives protection *in vitro*.

Results are shown in Fig. 2.3, it summarizes the whole set of antibodies screened, their binding sites on TeNT and their inhibitory activity. The last one was evaluated by following

the inhibition of the proteolytic activity of TeNT on CGNs. The use of cultured cerebellum granular neurons offers a simple and rapid way to screen the efficacy of each hu-mAb in inhibiting TeNT activity. The incubation with 1nM TeNT induces the cleavage of VAMP2 and its truncated form is then visualized by western blotting, revealed with a specific antibody. only five antibodies, from the whole set tested prevents the proteolytic activity in a concentration dependent manner. From this group of five hu-mAb, TT104.14 and TT110 resulted to be the best ones, giving a maximal protection at 2.5 nM and 0.5 nM, respectively.

***In vivo* screening: mouse lethality assay of TeNT with hu-mAb TT104.14 and TT110.** We further investigated the two hu-mAb, testing their inhibitory effect also *in vivo*. A wide range of doses from 2 pg/g to 20 pg/g was administered via intraperitoneal injections in mice. The antibodies were well tolerated by mice. The lethality of TeNT was evaluated in preliminary experiments, and a dose of 4 pg/g was sufficient to progressively induce classical symptoms of tetanus (generalized weakness, spasms limb muscle, labored breathing) and cause the deadly respiratory failure post injection.
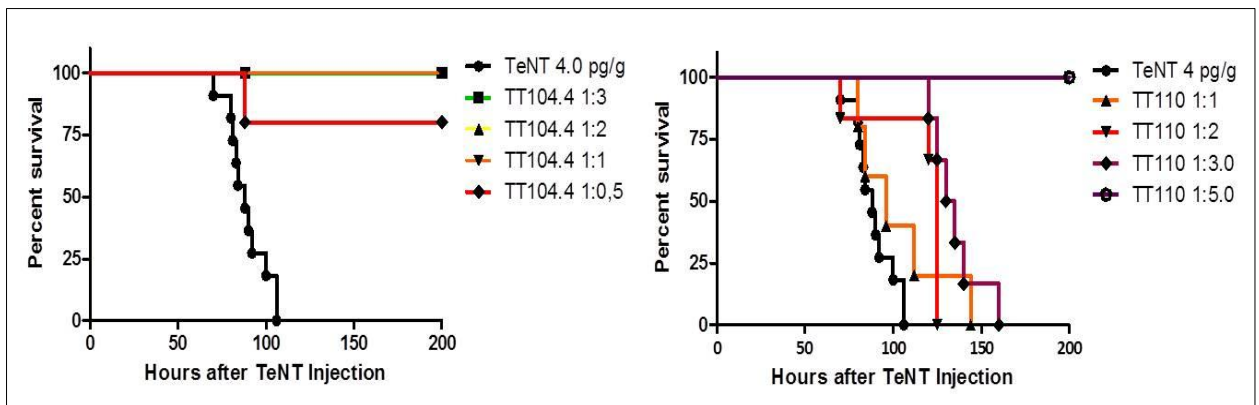

Fig. 2.4: Mouse lethality assay. The hu-mAbs tested delay and strongly protect mice against death induced by TeNT. Adult CD1 mice injected with 4pg/G TeNT, previously incubated with hu-mAbs at different ratios. For each condition n=9 mice were used. The animal were monitored every day. (A) The survival curve of hu-mAb TT104.4. (B) The survival curve of hu-mAb TT110.

The traces of Figure 2.4 (panel A) show that hu-mAb TT104,14 against the binding domain completely blocks the TeNT proteolytic activity to at least 1:1 ratio. Instead, the hu-mAb TT110 specific to the translocation domain, completely block the TeNT action at 1:5 ratio. An explanation for such different ratio between the two antibodies could be that for blocking the toxin action at the step of translocation requires more antibody, because the toxin is already inserted into the membrane of the vesicular compartment.

In vitro **binding of Fabs with TeNT, binary complex formation.** Having established the *in vitro* and *in vivo* inhibitory activity of the two hu-mAbs, we focused on the antibody fragments (Fabs) of the two identified hu-mAbs. This, considering that the aim of my work was to perform structural studies on TeNT, by using "chaperon molecules" to aid structural determination. Native antibodies are not suitable for co-crystallization attemps. They have flexible linker regions connecting the variable and constant domains (Figure 2.5, A). Monovalent antibody can be generated by proteolytic cleavage of the whole antibody, producing the two Fab fragments per antibody molecule (Figure 2.5, B). Recombinant antibody fragments are more versatile. They can be obtained by cloning the encoding genes from hybridoma cell lines, as well as by direct selection of recombinant antibody fragments from phage display libraries or by ribosome display. Up to now, all antibody fragments successfully used from co-crystallization are derived from hybridoma cell lines. So, the approach utilized for the crystallization studies of TeNT was that of using the antibody fragments as tools for stabilizing functionally relevant states of the protein. A binder target-protein complex has an enhanced chance to crystallize when a particular target protein conformation is stabilized. This is an approach very well supported in literature, in particular for membrane proteins, whose crystallization is quite difficult (Hunte, 2002; Röthlisberger *et al*., 2004; Griffin and Lawson, 2011; Bukowska and Grütter, 2013).
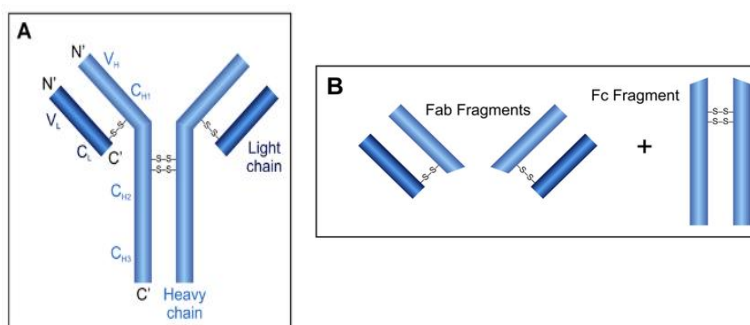

Fig. 2.5: Antibody scheme. An antibody molecule is composed by two heavy chains (H) of 50 kDa each, and two light chains (L) of 23 kDa each (A). Linked together by disulfide bonds and non-covalent interactions in a Y formation. Proteolytic cleavage of an antibody can produce two Fab fragments and a Fc fragment.

We focused on the biochemical analysis of the complex formed between TeNT and Fabs, (Fab104.14 corresponding to the hu-mAb TT104.4; Fab110 corresponding to hu-mAb TT110). From preliminary experiments we found that the best conditions for an *in vitro* reaction are the following: molar ratio 1:1 (TeNT:Fabs), incubation at 4°C overnight, stiring. The binary

complex formation was confirmed by a Native-PAGE analysis, which allows to detect proteins that retains their folded conformation (Figure 2.6). It is an excellent tool to detect binding events (protein-protein or protein- ligand). In our case we have a protein-protein interaction, that originates two binary complexes of 200kDa (TeNT-Fab104.14; TeNT-Fab110). The Native-PAGE analysis, clearly shows a molecular shift when TeNT and Fabs are putted together. Moreover, form the gel it seems that for the binary complex formation is necessary even less Fab, less than 1:1 molar ratio. Meanwhile the band of Fab110 is clearly evident in native gel, the one of Fab104.14 is not. This may be due to its intrinsic properties (charges and hydrodynamic size). But, the fact that a band corresponding to 200 kDa molecular weight is evident even when Fab104.14 is added, we conclude that also the binary complex TeNT-Fab104.14 is formed.
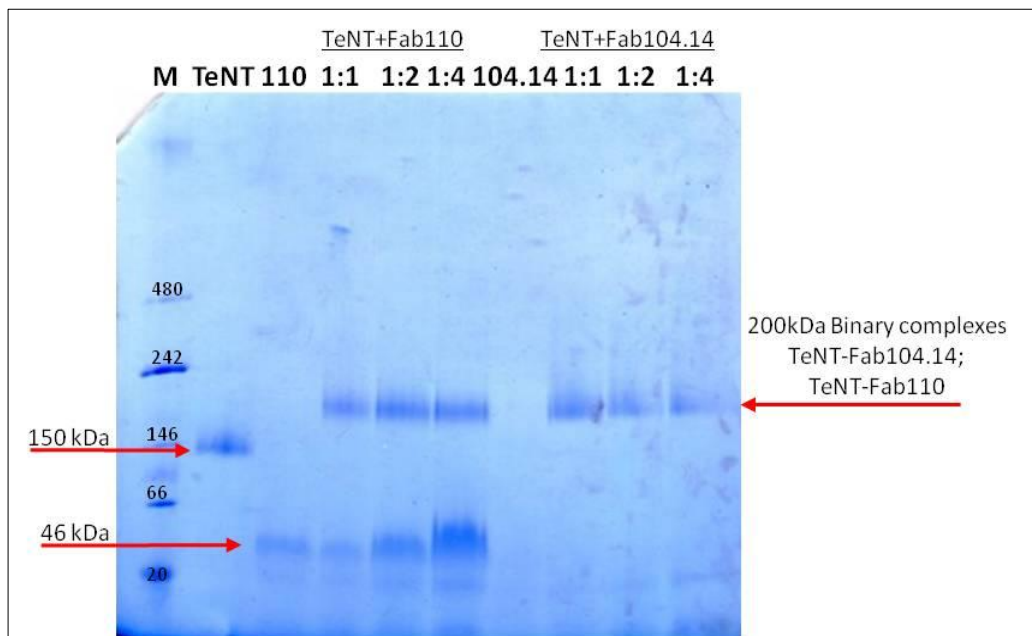

Fig. 2.6: Native-PAGE analysis of _in vitro_ reactions between TeNT and Fabs. In the first lane 5 ug of NativeMark[TM] unstained protein standard (ThermoFischer Scientific); second lane 1 ug of TeNT, 150 kDa; third lane 1 ug of Fab110, 46 kDa; lanes from 4 to 6, reactions of TeNT-Fab110 of three different molar ratios; seventh lane 1 ug Fab104.14, 46 kDa; lane from 8 to 10, reaction of TeNT-Fab104.14 of three different molar ratios.

Size exclusion chromatography (SEC) of the binary complexes. The fractions containing both binary complexes were pulled and concentrated until 500 µl, and subsequently loaded on Superdex 200 10/30 gel filtration column. This purification step has a triple function: it serves to remove the unbound Fabs, exploiting the difference in molecular weight, it allows us to see what is the state of our protein, whether aggregated or monodisperse. Furthermore, the gel filtration can determine whether the protein complex TeNT-Fab is stable in solution since a stable complex elutes as a single peak containing the two species. As we can seen from the chromatogram there are two peaks (Figure 2.7, A and B): the main peak at 11 (or 11.5) elution volume and a second peak at 15 ml elution volume. Two samples corresponding to the first peak, and to the second were loaded onto SDS-PAGE gel to determine its composition. The gel shows that in the peak are present both TeNT and Fab, which firmly elute as a single molecular specie, instead in the second peak is present the unbound Fab. For the first time we see a TeNT-Fab complex non aggregated and we have a second evidence that the Fabs are able to directly interact with TeNT *in vitro*. A fraction from the first peak of each binary complex was also loaded onto NATIVE-PAGE gel to further confirm complex formation (Figure 2.7, C).
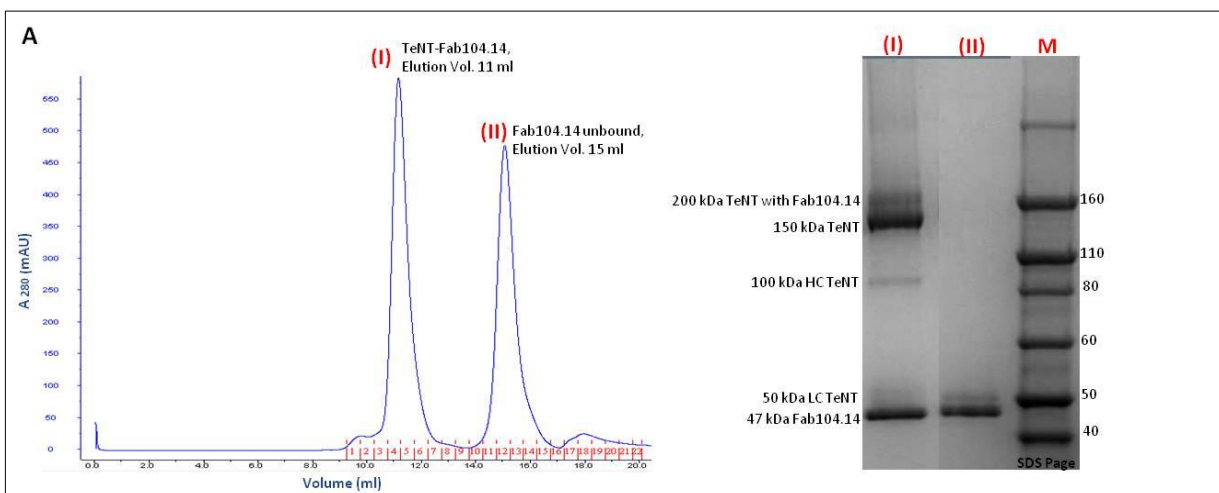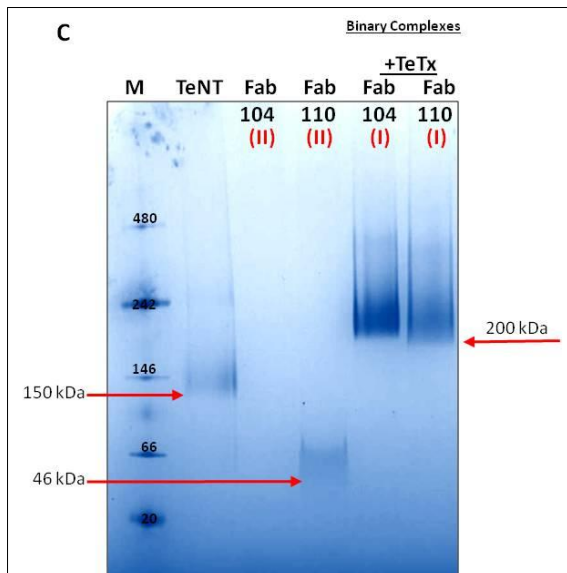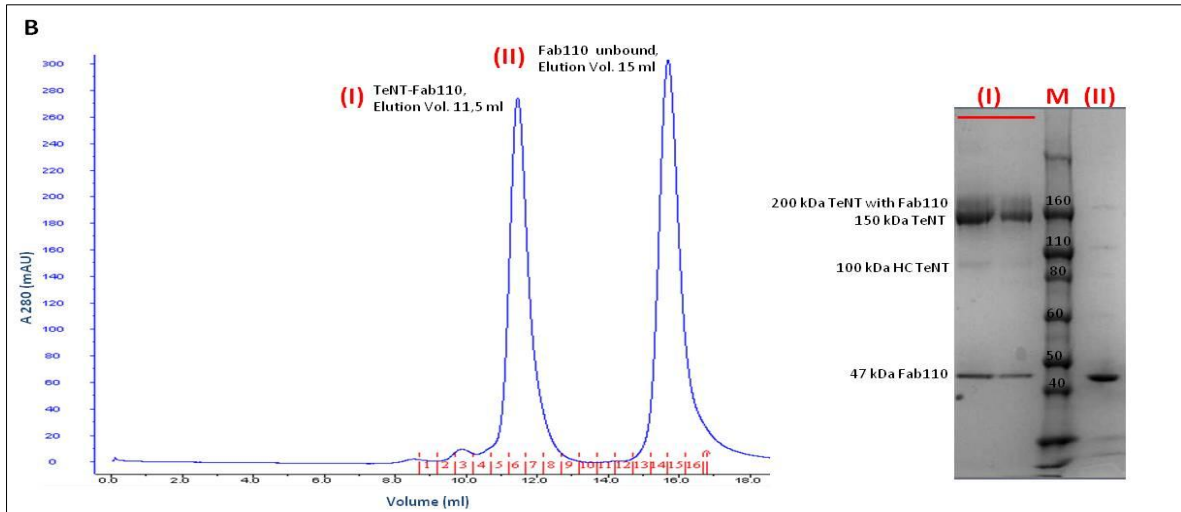
Fig. 2.7: Size exclusion chromatography of binary complexes. In blue absorbance at 280 nm. (A) SEC of TeNT- Fab104.14 binary complex. On the left SDS-PAGE. It shows that in peak (I) are present both TeNT and Fab104.14, and in peak (II) unbounded Fab104.14. (B) SEC of TeNT-Fab110 binary complex. The same as for Fab104.14. (C) Native-PAGE gel of the peaks from the SEC analysis of the both binary complexes. First lane Marker (kDa), second lane TeNT as control, lane 3 and 4, Fab104.14 and Fab110, lane 5 and 6 the binary complexes. We can appreciate the molecular shift of the binary complexes respect to TeNT alone.

Considering that SEC separates molecules according to their differences in size, we could appreciate the molecular shift from TeNT alone to TeNT-Fab, even with SEC analysis. The binary complexes elute earlier compared to the TeNT alone, with an elution volume that corresponds to a stable oligomer of 200 kDa (Figure 2.8). The same result was obtained also for the TeNT-Fab110 binary complex (data not shown).
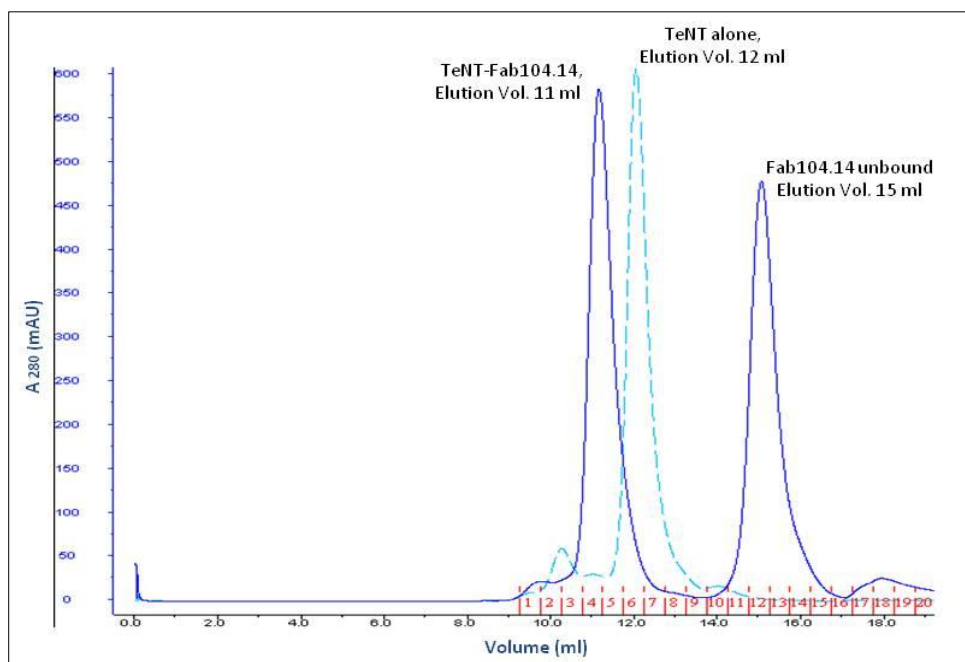
Fig. 2.8: Size exclusion chromatography of binary complexes. In blue absorbance at 280 nm. SEC of TeNT-Fab104.14 binary complex compared to TeNT alone, shown with dotted chromatogram.

SEC and NATIVE-PAGE analysis of the ternary complex TeNT-FaB104.14-Fab110. We then wondered if by putting together TeNT with both Fab molecules, we could obtain a stable ternary complex, as for the binary ones. In this way, all the two Fabs together, will be able to stabilize the inherent protein flexibility, as well as maintain one constant isoform of TeNT during the crystallization process, so favouring it. We used the same reaction conditions, as for the binary complexes. Molar ratio 1:1:1 (TeNT:Fab104.14:Fab110), overnight at 4°C, shaking. The next day the fraction containing the ternary complex were pulled and concentrated until 500 µl, and subsequently loaded on Superdex 200 10/30 gel filtration column. As we can seen from the chromatogram there are two peaks (Figure 2.9, A): the main peak at 10.2 ml and a second peak at 15 ml elution volume. Two samples corresponding to the first peak and to the second were loaded onto SDS-PAGE gel to determine its composition. The gel shows that in the peak are present both TeNT, Fab104.14 and Fab110 which firmly elute as a single molecular specie, instead in the second peak are present the unbound Fabs, that elutes at the same elution volume due to the same molecular weight (data not shown). Native-PAGE analysis also clearly showed that the main peak corresponds to a ternary complex of 250 kDa (Figure 2.9, C). If we compare the main peak of the ternary complex with the one of the binary complex, we can observe that it is slightly shifted, and elutes earlier. Thus, corresponding to a stable oligomer of 250 kDa (Figure 2.9, B).

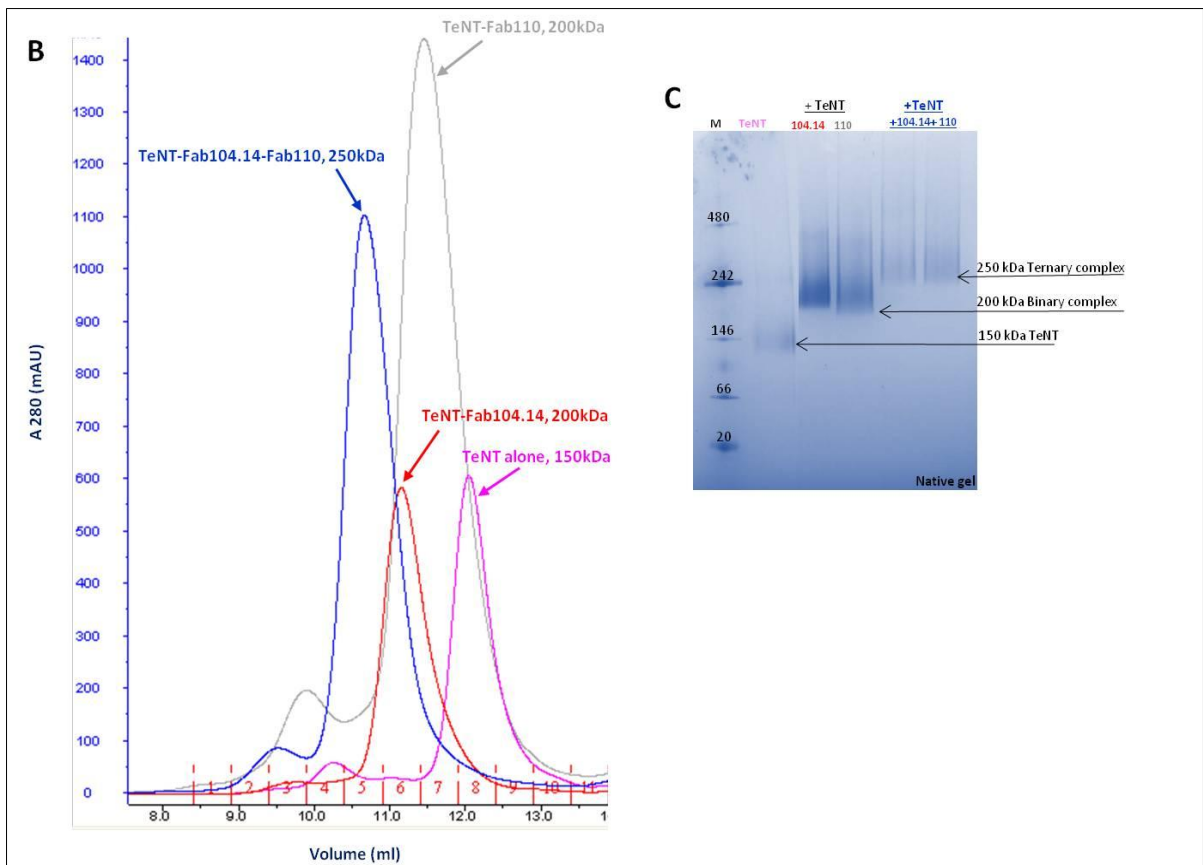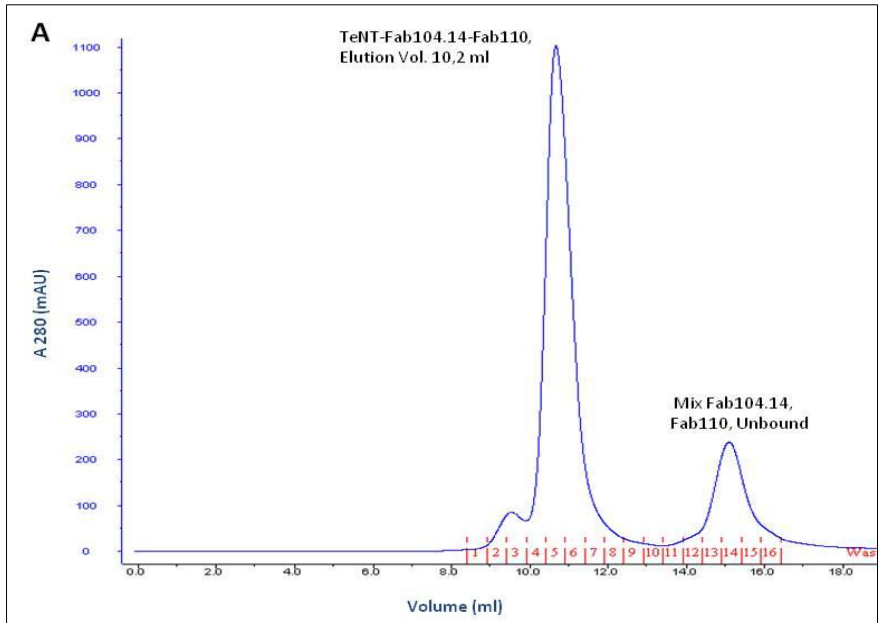**Fig. 2.9: Size exclusion chromatography of the ternary complex.** In blue absorbance at 280 nm. (A) SEC of TeNT-Fab104.14-Fab110 ternary complex. (B) SEC of ternary complex (Elution Vol. 10.2 ml) compared with the binary complexes (TeNT-Fab104.14 in red. Elution Vol. 11 ml; and TeNT-Fab110 in grey. Elution Vol. 11.5), and with TeNT alone in pink.Elution Vol. 12 ml. (C) Native-PAGE gel of both binary and ternary complexes.

Mouse lethality assay of the ternary complex. At this point, we wanted to see whether the analysed binary and ternary complexes, were able to protect mice from tetanus infection. Mouse lethality assays with binary and ternary complexes are shown in Figure 2.10, using lethality of TeNT as control. The mouse lethality assay of TeNTs with Fabs closely looks like the one of TeNT with the respective hu-mAbs. In fact, both binary complexes of TeNT with Fabs and the ternary one give a complete protection *in vivo.* This clearly indicates, that not only the interaction TeNT with single Fabs, but also the one with the Fabs together is quite stable and strong.
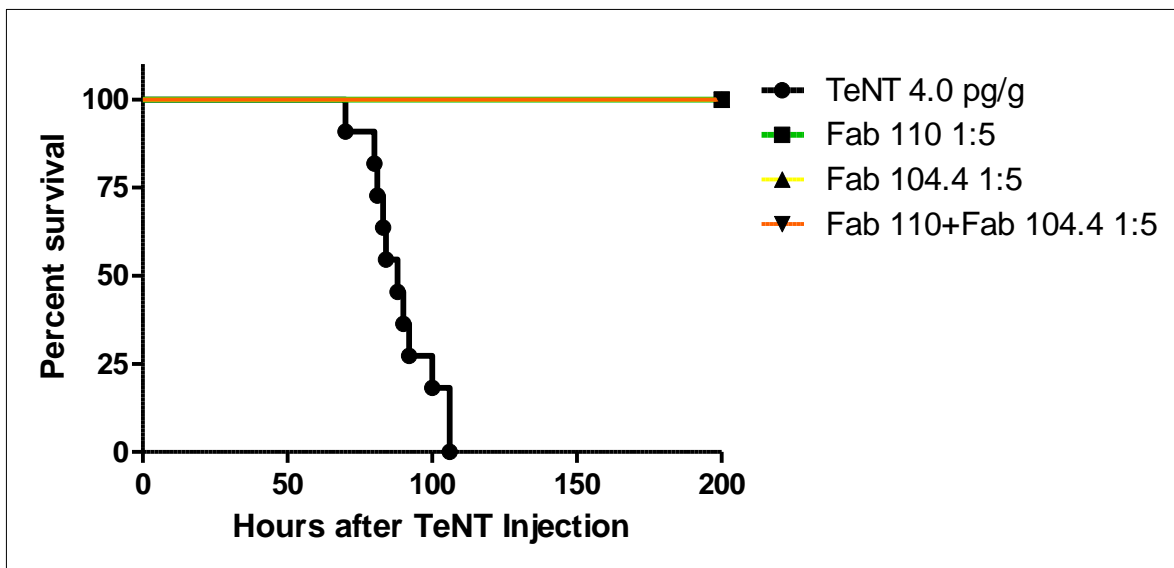

Fig. 2.10: Mouse lethality assay. The binary complexes tested delay and strongly protect mice against death induced by TeNT. Adult CD1 mice injected with 4pg/G TeNT, previously incubated with Fabs. In the figure is shown the 1:5 ratio (TeNT:Fabs), which gave the best result. For each condition n=9 mice were used. The animals were monitored every day (for 1 week).

4. CONCLUSIONS

Tetanus toxin (TeNT) is one of the most poisonous molecules known, the causative agent of the neuroparalytic disease tetanus. It acts on the central nervous system by blocking the neurotransmitter release and causing spastic paralysis. Although a lot is known about its domain organization and mechanism of action, no three dimensional structure is yet available. Instead experimental three-dimensional structures has been resolved for the N-terminal catalytic domain and C-terminal binding domain. Its crystallization has been proven to be quite difficult. This probably is due to some intrinsic properties of the toxin, not easy for us to be identified and that does not allow the crystallization process to occur. A crystal structure analysis will provide a tremendous amount of insights into both the structure and function of the protein. Moreover, an understanding of the molecular mechanism at the atomic level is a prerequisite for the development of an effective structure-based vaccine to treat tetanus victims. This part of my thesis work was aimed in understanding the biochemistry of the tetanus neurotoxin through crystallization studies.

The approach considered in order to have a suitable TeNT protein for crystallization, was that of using antibody fragments (Fabs) as tools for stabilizing functionally relevant states of the protein. A binder target-protein complex has an enhanced chance to crystallize when a particular target protein conformation is stabilized, and the Fabs are quite appropriate. The choice of the two Fabs (Fab104,14- that binds the binding domain of TeNT, and Fab104- that binds the translocation domain of the toxin) was done in the basis of previous results obtained by screening a set of human monoclonal antibodies. Two of these antibodies resulted to be very efficient in protecting mice from tetanus infection. So the Fabs that we used derived from these two antibodies.

First we tested the *in vitro* binding of the two chosen Fabs with the tetanus toxin. An overnight reaction was performed at 1:1 molar ratio and the samples analysed through a native page gel, in order to detect the complex formation. Gel-filtration experiments show co-elution of the TeNT with the respective Fabs, Fab104.14 and Fab110. We were able to to reconstitute *in vitro* a stable and pure TeNT-Fab104.14 and TeNT-Fab110 binary complex. The obtained binary complexes are also active *in vivo*, by protecting mice from tetanus. Different crystallization trials were done with the purified TeNT-Fabs complex.

The isolation of the ternary complex TeNT-Fab104.14-Fab110 was another result that allowed us to demonstrate that the interaction between the two Fabs together and TeNT can be

reproduced *in vitro*. The size exclusion chromatography showed that the ternary complex elutes as stable oligomer, indicating that also the two Fabs together are good protein partners required for TeNT stabilization. The ternary complex was tested *in vivo*, and it gives a complete protection. Even in this case several crystallization trials were done with the purified ternary complex

A huge amount of crystallization screening were performed, but yet we have not obtained good crystals for the study of the experimental three dimensional structure of TeNT. Preliminary data from electron microscopy negative staining reveal different conformations and heterogeneity of the purified ternary complex, and probably this may be one of the reasons why we still have not obtained any crystals. Work in progress in order to have an homogeneity of the purified binary and ternary complexes.

5. REFERENCES

1. Johnson EA. Clostridial toxins as therapeutic agents: benefits of nature's most toxic proteins. Annu Rev Microbiol. 1999; 53: 551-75.

2. Pellizzari R, Rossetto O, Schiavo G, Montecucco C. Tetanus and botulinum neurotoxins: mechanism of action and therapeutic uses. Philos Trans R Soc Lond B Biol Sci. 1999 Feb 28; 354(1381): 259-68.

3. Schiavo G, Poulain B, Rossetto O, Benfenati F, Tauc L, Montecucco C. Tetanus toxin is a zinc protein and its inhibition of neurotransmitter release and protease activity depend on zinc. EMBO J. 1992 Oct; 11(10): 3577-83.

4. Schiavo G, Benfenati F, Poulain B, Rossetto O, Polverino de Laureto P, DasGupta BR, Montecucco C. Tetanus and botulinum-B neurotoxins block neurotransmitter release by proteolytic cleavage of synaptobrevin. Nature. 1992 Oct 29; 359(6398): 832-5.

5. Lalli G, Herreros J, Osborne SL, Montecucco C, Rossetto O, Schiavo G. Functional characterisation of tetanus and botulinum neurotoxins binding domains. J Cell Sci. 1999 Aug; 112 (Pt 16): 2715-24.

6. Emsley P, Fotinou C, Black I, Fairweather NF, Charles IG, Watts C, Hewitt E, Isaacs NW. The structures of the H(C) fragment of tetanus toxin with carbohydrate subunit complexes provide insight into ganglioside binding. J Biol Chem. 2000 Mar24; 275(12): 8889-94.

7. Fotinou C, Emsley P, Black I, Ando H, Ishida H, Kiso M, Sinha KA, Fairweather NF, Isaacs NW. The crystal structure of tetanus toxin Hc fragment complexed with a synthetic GT1b analogue suggests cross-linking between ganglioside receptorsand the toxin. J Biol Chem. 2001 Aug 24; 276(34): 32274-81.

8. Brunger AT, Rummel A. Receptor and substrate interactions of clostridial neurotoxins. Toxicon. 2009 Oct; 54(5): 550-60.

9. Mocchetti I. Exogenous gangliosides, neuronal plasticity and repair, and the neurotrophins. Cell Mol Life Sci. 2005 Oct; 62(19-20): 2283-94.

10. Louch HA, Buczko ES, Woody MA, Venable RM, Vann WF. Identification of a binding site for ganglioside on the receptor binding domain of tetanus toxin. Biochemistry. 2002 Nov 19; 41(46): 13644-52.

11. Bercsenyi K, Schmieg N, Bryson JB, Wallace M, Caccin P, Golding M, Zanotti G,Greensmith L, Nischt R, Schiavo G. Tetanus toxin entry. Nidogens are therapeutic targets for the prevention of tetanus. Science. 2014 Nov 28; 346(6213): 1118-23.

12. Herreros J, Ng T, Schiavo G. Lipid rafts act as specialized domains for tetanus toxin binding and internalization into neurons. Mol Biol Cell. 2001 Oct; 12(10): 2947-60.

13. Lacy DB, Stevens RC. Unraveling the structures and modes of action of bacterial toxins. Curr Opin Struct Biol. 1998 Dec; 8(6): 778-84.

14. Sheridan RE. Gating and permeability of ion channels produced by botulinum toxin types A and E in PC12 cell membranes. Toxicon. 1998 May; 36(5): 703-17.

15. Blaustein RO, Germann WJ, Finkelstein A, DasGupta BR. The N-terminal half of the heavy chain of botulinum type A neurotoxin forms channels in planar phospholipid bilayers. FEBS Lett. 1987 Dec 21; 226(1): 115-20.

16. Breidenbach MA, Brunger AT. 2.3 A crystal structure of tetanus neurotoxin light chain. Biochemistry. 2005 May 24; 44(20): 7450-7.

17. Rao KN, Kumaran D, Binz T, Swaminathan S. Structural analysis of the catalytic domain of tetanus neurotoxin. Toxicon. 2005 Jun 1; 45(7): 929-39.

18. Lacy DB, Tepp W, Cohen AC, DasGupta BR, Stevens RC. Crystal structure of botulinum neurotoxin type A and implications for toxicity. Nat Struct Biol. 1998 Oct; 5(10): 898-902.

19. Swaminathan S, Eswaramoorthy S. Structural analysis of the catalytic and binding sites of Clostridium botulinum neurotoxin B. Nat Struct Biol. 2000 Aug; 7(8): 693-9.

20. Kumaran D, Eswaramoorthy S, Furey W, Navaza J, Sax M, Swaminathan S. Domain organization in Clostridium botulinum neurotoxin type E is unique: its implication in faster translocation. J Mol Biol. 2009 Feb 13; 386(1): 233-45.

21. Hunte C, Michel H. Crystallisation of membrane proteins mediated by antibody fragments. Curr Opin Struct Biol. 2002 Aug; 12(4): 503-8.

22. Röthlisberger D, Pos KM, Plückthun A. An antibody library for stabilizing and crystallizing membrane proteins - selecting binders to the citrate carrier CitS. FEBS Lett. 2004 Apr 30; 564(3): 340-8.

23. Griffin L, Lawson A. Antibody fragments as tools in crystallography. Clin Exp Immunol. 2011 Sep; 165(3): 285-91.

24. Bukowska MA, Grütter MG. New concepts and aids to facilitate crystallization. Curr Opin Struct Biol. 2013 Jun; 23(3): 409-16.

PART III

**FUNCTIONAL ANALYSIS OF BOTULINUM NEUROTOXIN TRAFFICKING
AT THE NEUROMUSCULAR JUNCTION**

PART III: FUNCTIONAL ANALYSIS OF BOTULINUM NEUROTOXIN TRAFFICKING AT THE NEUROMUSCULAR JUNCTION

1. INTRODUCTION

1.1 Botulinum neurotoxins: molecular structure and mechanism of action

Botulinum neurotoxins (BoNTs) are bacterial protein produced by *Clostridium botulinum* strains and are the most hazardous toxins known up to now. They block the release of neurotransmitters from synaptic vesicles and act in nanogram quantities because of their ability to specifically target neurons (Gill, 1982). The botulinum neurotoxins are produced in dozens of different isoforms, grouped into eight distinct serotypes (BoNT/A to /H) that exhibit amino acid sequence conservation. BoNTs are structurally organized in two main chains: a light chain (L, 50 KDa) and a heavy chain (H, 100 KDa) held together by a strictly conserved inter-chain disulfide bond and non-covalent interactions (Rossetto *et al.,* 2014; Rummel, 2015). These two chains based on their functional properties are organised in four domains (Figure 3.1): (I) HC-C (25 kDa, in green) is involved in nerve terminal binding and internalization (Montecucco, 1986; Binz and Rummel, 2009; Brunger and Rummel, 2009; Rummel, 2013;); (ii) HC-N (25 kDa, in purple), as not yet a well-defined role, but it is prpopsed that it may contribute to binding by interacting with membrane lipids (Muraro *et al.,* 2009; Ayyar *et al.,* 2015; Zhang *et al.,* 2012) (iii) HN (50 kDa, in yellow) assists the translocation of the catalytic part of the toxin from the internal part of an intracellular acidic compartment into the cytosol (Fischer and Montal, 2007; Montal, 2010; Pirazzini *et al.,* 2015); (iv) the L catalytic domain (50 kDa, in red) is a metalloprotease that cleaves the SNARE proteins interfering with the release of neurotransmitters that result in a reversible neuroparalysis (Pantano *et al.,* 2013). Despite the amino acid sequence variability among all BoNT variants, the structure organization is however maintained, as it mechanism of nerve intoxication (Pantano *et al.,* 2013). The domain organization of BoNTs is closely related to their mechanism of action: (i) functional binding to polysialogangliosides (PSG), highly enriched in the neuromuscular junction (NMJ); (ii) membrane translocation across the SV membrane driven by a pH lowering, which is physiologically necessary for the neurotransmitter refilling of these compartments; (iii) metalloproteolytic activity specific for VAMP, SNAP-25, or syntaxin, three proteins that are members of machinery for the

neurotransmitter release. In the following sections, will be reviewed more in details relevant insight concerning BoNTs mechanism of action.
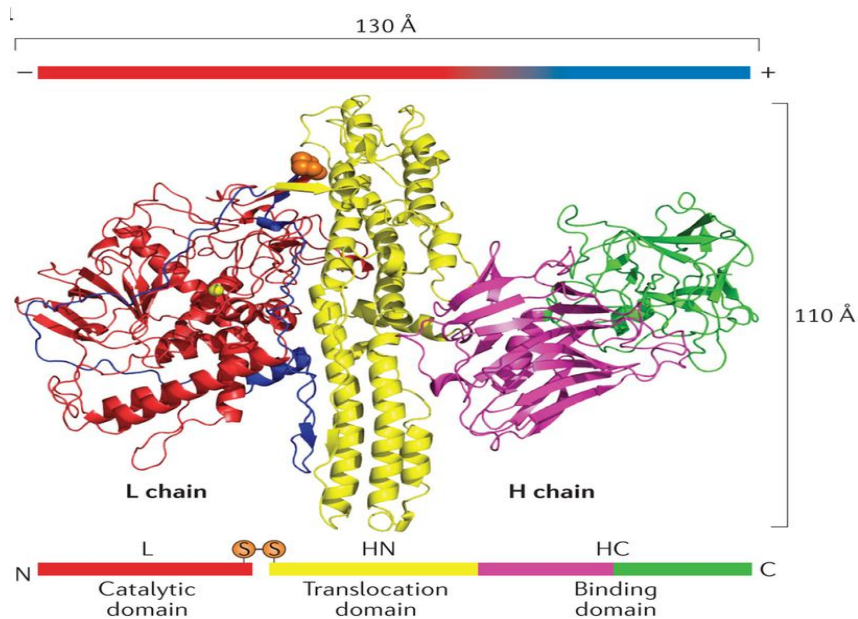

Fig. 3.1: Crystallographic structure of isolated BoNT/A1. Crystal structure of botulinum neurotoxin A1 (BoNT/A1) (PDB 3BTA), showing its organization of individual toxin domains, every of that with a specific role in cellular mechanism of intoxication: the HC domain binds specifically to the nerve terminals; the HN domain translocate the L chain into the cytosol of the nerve terminal; and L chain is a metalloprotease that cleaves specific SNARE proteins, involved in neurotransmitter release, thereby causing neuroparalysis. A peptide belt (showing in dark blue), that surrounds the L domain and the inter-chain disulfide bond (orange), links the L chain to the HN domain. From Rossetto *et al.,* 2014.

Membrane binding and the "dual receptor model". The high potency of BoNTs is mainly due to their neurospecific binding which is mediated by the interaction with two receptor components. The double receptor model is based on a first binding to a polysialoganglioside molecule followed by a second interaction with a protein receptor (Montecucco, 1986). Indeed, BoNTs have evolved this ability to bind neurons via two receptors, one with low affinity, a polysialogangliosides (PSG), that increases toxin density on the target membrane (Binz and Rummel, 2009; Rummel, 2013), and a secondary one the luminal part of an integral membrane protein of synaptic vesicles (SV), which triggers the internalization into the endocytic pathway (Matteoli *et al.,* 1996) (Figure 3.2).

More in detail, gangliosides are a large family of glycosphingolipids present on the external plasma membrane of cells and are involved in many pathways like cell signalling, protein sorting and are very important for membrane domain formation and organization.

Gangliosides are particularly enriched in neurons membrane, especially in axons and dendrites where they govern membrane curvature (Ledeen *et al.,* 1993; Sonnino *et al.,* 2007). Indeed, this binding of BoNTs to the negatively charged sialic acids of PSG is very efficient because these neurotoxins are dipoles, with their positively charged end situated close to the binding site. This effect contributes not only to the rapid binding of BoNTs to the nerve terminal *in vivo*, but also to their reorientation that allow the interaction with the second receptor. The PSG-binding site of BoNT/A, /B, /E, /F and /G, is located in the HC-C domain, outlined by the conserved motif E(or D or Q)...H(or K or G)...SXWY...G (where X is any amino acid and "..." denotes a variable. Also, the PSG-binding site for BoNT/C, BoNT/DC and BoNT/D is found in a similar position, but the binding motif is different (Karalewitz *et al.,* 2010; Strotmeier *et al.,* 2010; Zhang *et al.,* 2010; Karalewitz *et al*., 2012).

Subsequently, upon exocytosis the intralumenal domains of the synaptic vesicle proteins are exposed and can be accessed by the surface attached neurotoxins. BoNT/B, BoNT/G and BoNT/DC bind with their HC-C domain to the lumenal domain of synaptotagmin-I/II (Syt-I, Syt-II) (Nishiki *et al.,* 1994; Nishiki *et al.,* 1996; Dong *et al.,* 2003; Rummel *et al.,* 2004; Mahrhold *et al.,* 2006; Chai *et al.,* 2006; Jin *et al.,* 2006; Dong *et al.,* 2007; Peng *et al.,* 2012; Bertnsson *et al.,* 2013; Willjes *et al.,* 2013). By contrast, BoNT/A and BoNT/E bind specifically to two different segments of the fourth lumenal loop of the synaptic vesicle transmembrane protein SV2 (Dong *et aL*., 2006; Dong *et al.,* 2008; Benoit *et al.,* 2014). SV2C appears to be the main receptor involved in BoNT/A binding, while SV2A e SV2B, but not SV2C, mediate BoNT/E entry. However all three isoforms are expressed in motoneurons (Benoit *et al.,* 2014). The protein receptors of other BoNTs have not been yet fully characterized, although SV2A-C seems to play an important role in the uptake mechanism of BoNT/D and BoNT/F (Fu *et al.,* 2009; Rummel *et al.,* 2009; Peng *et al.,* 2011; Rummel, 2015).

Thereafter the synaptic vesicle is recycled and the anchored BoNT is endocytosed. Acidification of the vesicle lumen triggers membrane insertion of the translocation domain followed by pore formation and translocation of the enzymatically light chain to its site of action.

Previously in our laboratory, BoNT/A was visualized for the first time inside small clear synaptic vesicles present within the motor nerve terminal of the neuromuscular junction (NMJ). It was demonstrated that the translocation of BoNT/A takes place from synaptic vesicles and not from the endosomal compartment (Colasante *et al.,* 2013). The mechanism

of internalization of other BoNTs remains to be established. By contrast in cultured neuron and probably also *in vivo*, alternative vesicles and trafficking route may contribute to their entry (Pellet *et al.,* 2015). Indeed, information concerning the nature of the endocytic vesicle involved in the uptake of the other serotypes is still lacking. In this thesis, we will discuss about the possible distinctive trafficking exploited by different serotypes of BoNTs. Indeed, we show a different immunoflourescence staining between the different serotypes tested during binding and internalization.
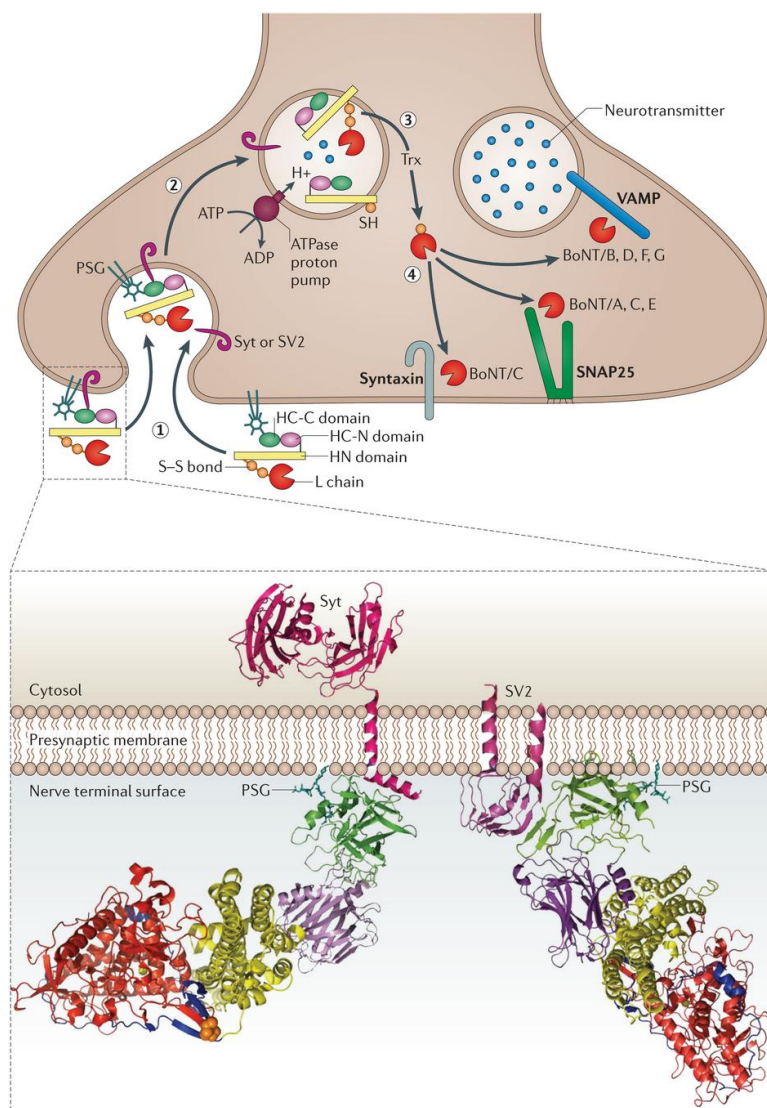

Fig. 3.2: Botulinum neurotoxins mechanism of action within peripheral nerve terminals. The BoNT mechanism of action starts with a primary interaction between the HC-C domain and a polysialogangliosides (PSG). Subsequent lateral movements make possible the binding of the toxin with a protein receptor which is the lumenal domain of a synaptic vesicle protein (step 1). The protein receptor has been identified as synaptotagmin I and II for BoNT/B, /DC and /G (crystal structure shown on the lower left-hand side), and SV2 for

BoNT/A, /E and /F (crystal structure shown on the right left-hand side); the protein receptor for the remaining serotypesis still unknown and it remains to be clarified. This latter binding to the protein receptor is fundamental for the internalization of the toxin-receptors complex inside an acidic intracellular compartment (step 2) whose nature has been identified as SV for BoNT/A1 (Colasante *et al.,* 2014). Little is known on the nature of endocytic compartments exploited by the other BoNT serotypes, however several evidences show that the acidification of its lumen triggers a structural rearrangement of L chain and the translocation domain (HN) (step 3). This process ends with the reduction of the disulfide bond performed by the thioredoxin reductase-thioredoxin system. The free L metalloproteases can now cleave one of the three SNARE proteins (step 4) thereby preventing Ca^{2+} elicited release of the neurotransmitter contained insides SV. From Rossetto *et al.,* 2014.

Translocation across the membrane of acidic intracellular compartments. Considering the steps of BoNTs cellular mechanism of intoxication in nerve terminals, the membrane translocation of the L chain into the cytosol is the least understood in terms of molecular mechanism. BoNTs have evolved to use a relevant physiological feature of nerve terminals, they exploit the acidification of the synaptic vesicles (SV) lumen carried out by the v-ATPase, a proton pump present on their membrane (Sudhof, 2013), that lowers the lumenal pH to generate the pH gradient driving the re-uptake of neurotransmitters from the cytoplasm into SV (Pantano *et al.,* 2013; Pirazzini *et al.,* 2015). The importance of the v-ATPase in BoNTs mechanism of action, is extensively demonstrated by the fact that specific inhibitors block BoNTs neurotoxicity (Simpson *et al.,* 1994; Sun *et al.,* 2012).

Despite the fact that the exact molecular mechanism is still under debate, it is well known that the translocation step is mediated by a structural rearrangement of the entire molecule. Indeed it is long known that at acidic pH BoNTs forms ion conducting channels, and that this channel mediates the translocation of the L chain into the cytosol (Fisher and Montal, 2007; Montal, 2010; Koriazova and Montal, 2003; Fischer and Montal, 2013). Montal and colleagues gave the major contribution by using the patch clamp technique, and showing that the transmembrane ion channel formation in planar lipid bilayers is associated with the translocation of the L chain of BoNT/A1 with cleavage of its target protein, SNAP-25. The outcomes of these experiments are shown and interpreted with the model reported in Figure 3.3 (Montal, 2010; Fischer and Montal, 2013). The HN domain of BoNT/A (in yellow), when the pH is lowered on the *cis* side of the patched membrane (corresponding of the SV lumen), and when a negative membrane potential is applied, it forms a transmembrane channel that chaperons the passage of the L chain (in red) on the *trans* side (corresponding to cell cytosol).

The increasing of the transmembrane current begins with low values (~ 10 pS) corresponding to the phase during which the L chain occupies the channel to pass on the other side, and raises within 10 minutes to ~ 65 pS or ~ 110 pS, in PC12 cell line (Figure 3.2), thus corresponding to the full conductance of a transmembrane channel (Fischer and Montal, 2007; Fischer *et al.,* 2009; Montal, 2010; Fischer and Montal 2013). Interestingly, this formed channel permits the passage of only α-helices but not tertiary structure elements, indicating that the L chain has to unfold, at least partially, in order fit within the narrow cavity (15-20 Å in diameter) (Figure 3.3, B) (Montecucco, 1986; Kukreja *et al.,* 2006; Cai *et al.,* 2006; Montal, 2010).
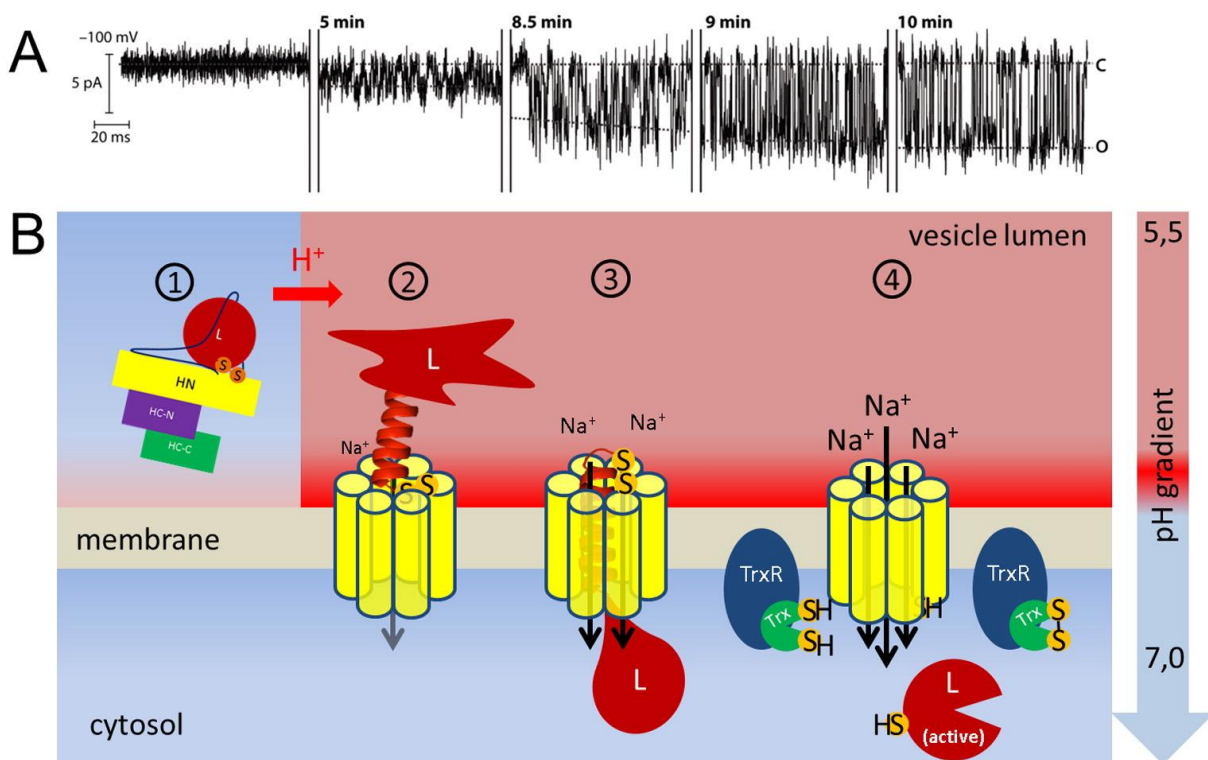

Fig. 3.3: Membrane translocation of BoNTs across the membrane of endocytic compartments. (A) The upper panel shows the increase of conductance of the plasma membrane at low pH in Neuro2A cell line, induced by BoNT/A1. (B) The lower panel shows steps proposed and involved in the membrane translocation of the L chain: 1) a schematic structure of the toxin; 2) the HN domain at acidic pH inserts into the membrane forming a transmembrane channel, hypothetically made of a six α –helices; 3) the translocation of L chain from the acidic lumen into the neutral cytosol increases the conductance; 4) complete translocation of the L chain within the cytosol where it refolds and the inter-chain disulfide bond is reduced by the Thioredoxin Reductase-Thioredoxin system. From Pirazzini *et al.,* 2015.

For a successful translocation mechanism, the disulfide bond must remain intact during the initial phase of the process, and must be reduced only when it reaches the trans-side of the

membrane. This data are in agreement with the fact that pre-reduced BoNT does not form channels and that the reduction at any stage before reaching the cytosolic side aborts channel formation and consequently L chain translocation (Fischer and Montal, 2007; Fischer and Montal, 2013). Thus the model proposed by Montal and co-workers, suggests the fact that upon acidification the BoNT molecules change their structure, HN inserts into the membrane and the L chain unfold maintaining only secondary structure elements. Thereafter L chain remains connected to the SV till the inter-chain disulfide bond is reduced, and that is the concluding step that conclude the process leaving the HN channel to its full conductance (Figure 3.3, A and B).

However, such a model does not take in account of other important data present in literature: i) data from the crystal structure of BoNT/B, and the L chain and HN domain of BoNT/A, show that they do not change structure at low pH in solution (Eswaramoorthy *et al.,* 2004; Galloux *et al.,* 2008), while they undergo conformational changes in the presence of PSG or lipids (Montecucco, 1986; Fu *et al.,* 2002; Puhar *et al.,* 2004; Sun *et al.,* 2011); ii) from membrane photolabelling studies that is bypassed the internalization step and induced the translocation of the L chain directly from the cell surface, it has been found that BoNTs are attached to the membrane by two receptors and that the membrane translocation occurs within few minutes at 37 °C in the pH range 4.5-6, this is consistent with the pH within the synaptic vesicle, and with the fact that very little translocation is taking place at 20 °C (Pirazzini *et al.,* 2011); iii) the replacement of three carboxylate residues with the corresponding amides in BoNT/B, doesn't allow their protonation, thus the L chain to enter the cytoplasm quicker, increasing toxicity (Pirazzini *et al.,* 2013).

All these data, taken together suggest that there is not only one single pH sensor in BoNTs, but several carboxylates that have high pKa values and play an important role in the low pH-driven release of the L chain into the cytosol.

An updated model for BoNT translocation has been proposed, shown in Figure 3.4. (Pirazzini *et al.,* 2014). BoNTs bind to its two receptors within the SV lumen, which initially has a neutral pH, immediately after endocytosis. Then, the v-ATPase pumps protons and SV lumen becomes progressively more acidic. There is no a single pH sensor in BoNTs, but the conserved carboxylates predicted to have higher pKa, get protonated, and drive the partially protonated BoNT toward the membrane surface involving the disulphide-containing face of the toxin. Here, the pH is more acidic with respect to the lumen allowing further protonation

of other carboxylates. The subsequent molecular events are currently unknown, but on the basis of earlier studies, it can be speculated that the L chain becomes a "molten globule", a protein state variant that retains native secondary structure and then it increases hydrophobicity, thus enabling its insertion and passage across the membrane (Pirazzini *et al.,* 2013; Rossetto *et al.,* 2014; Pirazzini *et al.,* 2015).

It has been proposed that the long α-helices of HN may break by generating amphipathic helices with the length of 20-24 residues that, together with the other amphipathic helices of the HN domain insert in the membrane, by forming a laterally opened transmembrane channel. The arc-shaped membrane inserted HN may have a function as chaperone for the translocation of the L chain, as suggested by Koriazova and Montal (Koriazova and Montal, 2003; Montal 2010; Fischer and Montal, 2013). By facing the neutral pH of the cytosol, the L chain of BoNTs deprotonates and refolds into the metalloprotease domain whilst the membrane inserted HN closes laterally to form a stable ion channel. The process is then closed by the reduction of the disulfide bridge, that releases the L chain and its protease activity, attaining the HN channel for its full conductance.
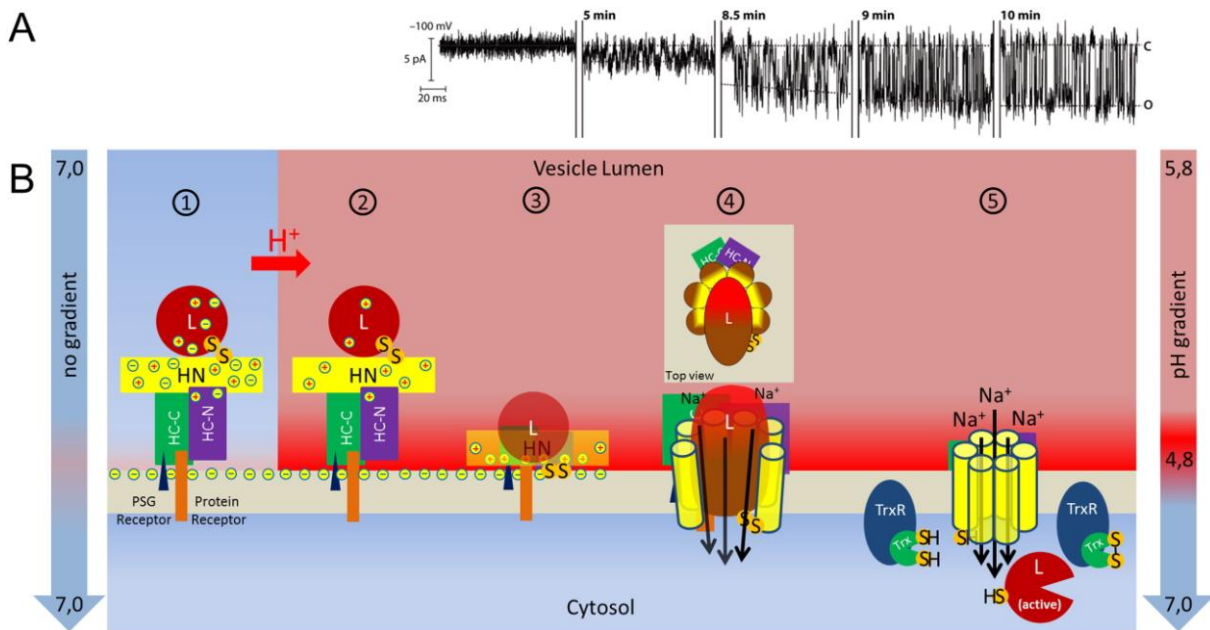
Fig. 3.4: A novel model proposed for the translocation step in botulinum mechanism of action . 1) Schematic representation of the four domains of the toxin in different colours: L (red), HN (yellow), HC-H (purple) and HC-C (green). The HC-C domain, binds to its two receptors: the polysialoganglioside (blue triangle) and the lumenal part of SV protein (SV2 or synaptotagmin, orange rectangle). 2) The v-ATPase protons pump and the vesicle lumen is acidified and the carboxylate residues are protonated. 4) A net positive charge is acquired by the protein at this face that can eventually fall down on the anionic membrane surface; low pH and lipid interaction

cause a combined and sequential structural. 5) L crosses to the cytosolic side, refolds and then is released upon reduction of the disulfide bridge. From Pirazzini *et al.,* 2015.

Whether the situation of the membrane translocation of BoNTs is actually as it was previously described is currently unknown. This last mechanism is a speculation and additional studies are needed to clarify this essential step and still unclear of the BoNT intoxication process.

The disulphide bond reduction. The interchain disulphide bond plays a functional role in cellular BoNTs intoxication. The first evidence was given by the lack of toxicity *in vivo* of previously reduced neurotoxin (Schiavo *et al.,* 1997). Fischer and Montal have demonstrated that for a successful translocation, the L chain has to remain linked to H via the inter-chain SS bridge and that its reduction is the concluding event, that which frees the L chain enabling the metalloprotease activity (Fischer and Montal, 2007). Indeed, the premature reduction of this bond, at any stage before its exposure to the cytoplasm, abolish the L chain translocation, thus indicating that it plays a fundamental role within the cellular intoxication process and that it has to reach intact the cytosolic side of the membrane (Pirazzini *et al.,* 2011; Rossetto *et al.,* 2014). All these data taken together indicate that the reduction of the interchain disulfide bond within nerve terminal cytosol may be a "*conditio sine qua non*" to the metalloprotease activity of BoNTs, thus representing a target for the development of mechanism-based antitoxins (Pirazzini *et al.,* 2015). The SV lumen of most intracellular organelle is oxidant, while the cell cytosol has a reducing potential, which is kept by a large number of redox couples (Arner and Holmgren, 2000; Holmgren *et al.,* 2010; Hanschmann *et al.,* 2013). The reduction of protein disulfides bonds is catalysed in the cell by several enzymatic systems. Two of which are the glutathione-glutaredoxin system and the NADPH-Thioredoxin reductase (TrxR)-Thioredoxin (Trx). It was demonstrated that the TrxR may be involved in the reduction of the interchain disulfide bond of BoNTs. It was found that Auranofin, the most potent TrxR inhibitor identified so far, prevented the toxicity of BoNT/B, /C and /D (Pirazzini *et al.,* 2013; Pirazzini *et al.,*2014). Instead, buthione sulfoximine, a compound that substantially reduce glutathione intracellular levels, had no inhibitory activity, indicating that the glutathione-glutaredoxin system is not involved in the entry of BoNTs in the cytoplasm (Pirazzini *et al.,*2013).

The L chains of BoNTs are metalloproteases specific for the SNARE proteins. Once that the L chain is free in the cytosol, it functions as a Zn^{2+} dependent endopeptidase that exclusively hydrolyses distinct peptide bonds of neuronal SNARE proteins: VAMP (vesicle-associated membrane protein; also called synaptobrevin), SNAP-25 (synaptosomal-associated protein of 25 kDa) or syntaxin which are cleaved at single sites. More in details, BoNT/A, and BoNT/E cleave SNAP25 (Schiavo *et al.,* 1993; Blasi *et al.,* 1993), BoNT/B, BoNT/D, BoNT/F and BoNT/G cleave VAMP (Schiavo *et al.,* 1992; Schiavo *et al.,* 1993), instead, BoNT/C is unique because cleave both SNAP25 and syntaxin (Pantano *et al.,* 2013). The inactivation of any of these three proteins inhibits the neurotransmitter release, this is the strongest evidence that the three SNARE proteins form the core of the neuroexocytosis nanomachine (Sutton *et al.,* 1998; Schiavo *et al.,* 2000; Binz, 2013; Pantano *et al.,* 2013). The SNARE family of proteins includes several isoforms and they are differentially expressed in many non-neuronal cells and tissues. BoNTs cleave SNARE proteins by removing large cytosolic segments, which prevents the formation of the SNARE complex. Instead, only BoNT/A and BoNT/C remove only a few residues from the C-terminal of SNAP-25 and, this SNAP-25 truncated form are still able to form a stable SNARE complex; thus, the molecular mechanism of BoNT/A and BoNT/C-induced neuroparalysis still remains to be clarified. The cleavage of a SNARE protein prevents the assembly of the SNARE complex, which is fundamental for the fusion of the vesicles containg the neurotransmitter, with the presynaptic membrane. As long as the L chain remains active, the nerve terminal remains paralysed.

Therefore, BoNTs can be used as tools to determine the effect of knocking-out specific proteins of the SNARE complex in cell physiology (Pantano *et al.,* 2013).

2. AIM OF THE WORK

Botulinum neurotoxins (BoNTs) are bacterial protein produced by *Clostridium botulinum* strains and are the most hazardous toxins known up to now. They block the release of neurotransmitters from synaptic vesicles and act in nanogram quantities because of their ability to specifically target neurons. Eight different serotypes are known, named A to H, and exhibit amino acid sequence conservation. BoNTs are peculiar with respect to their pre-synaptic membrane binding which is mediated by a polysialoganglioside and by a protein receptor consisting of the luminal portion of a synaptic vesicle membrane protein. BoNT/A, BoNT/E and BoNT/F bind to SV2, while BoNT/B, BoNT/G bind to synaptotagmin. To date the protein receptor of other BoNT serotypes, BoNT/C and D has not been conclusively determined. While the intoxication step has been clarified, endocytosis and membrane translocation remain largely unknown. The fact that the known BoNT receptors are in the luminal domain of synaptic vesicles strongly suggests that BoNTs are endocytosed inside synaptic vesicles at peripheral nerve terminals. However, their actual presence inside vesicles and the type of synaptic vesicles has not been determined. Using immunoelectron microscopy technique BoNT/A1 was visualized for the first time inside small clear synaptic vesicles present within the motor nerve terminal of the neuromuscular junction (NMJ).

Taken in consideration this, the aim of my work was to study the initial trafficking events for other BoNTs, in particular for BoNT/A5/B and BoNT/D. We focused on BoNT/A5 and /B because most frequently associated with human botulism, instead BoNT/D frequently associated with animal botulism. Also the choice of these BoNTs was due to the different time required for intoxication, BoNT/A5 and /D translocate their L-chain very rapidly, instead BoNT/B intoxication is longer. I have prepared the binding domains (HCs) of these BoNTs, which are both necessary and sufficient for binding to the neuronal surface and internalization. HC-BoNTs are considered ideal tools to exploit the initial trafficking of BoNTs intoxication. Each binding domain was prepared fused with and appropriate fluorescent tags in *E.coli*, in order to directly visualize their distribution at the NMJ using fluorescence microscopy.

3. MATERIAL AND METHODS

Animals. For in vivo experiments, adult male CD1/Swiss-Webster mice weighing 26-28g were used. Instead, for neuronal culture rats from 6- to 8-days-old were sacrified. All experiments were performed in accordance with the European Communities Council Directive n°2010/63/UE and approved by the Italian Ministry of Health.

Antibodies and reagents. Antibodies were obtained from the following sources: mouse anti-His tag (Novagen, #70796), rabbit anti GFP (Abcam, #6556), Alexa Flour-555 conjugated α-bungarotoxin (Invitrogen, #B3545). Flourescently conjugated secondary antibodies were obtained from Merck Millipore. The remaining reagents were sourced from Sigma unless stated otherwise.

Construction of the HC-BoNTs expression vectors. The DNA encoding the following HC-BoNTs: cp-YFP-HC-BoNT/A5 (residues 876-1296); mCherry-HC-BoNT/D (residues 863-1276); GFP-HC-BoNT/B (residues 832-1290) was synthesized (GeneArt Gene Synthesis, Thermo Fischer Scientific) with optimal codon bias for *Escherichia coli* expression. The DNA fragment was amplified and subcloned into unique BamHI and HindIII restriction sites of pET28a+ vector expression vector (Novagen) for HC-BoNT/A5 and /D. Instead, HC-BoNT/B was subcloned into unique XhoI and HindIII restriction sites of pRSETa expression vector (Thermo Fischer Scientific). Correct insertion of HC-BoNTs DNA was confermed by DNA sequencing at BMR Genomics (Padova). HC-BoNT/A5-pET28a+ and HC-BoNT/D-pET28a+ were tranfromed into BL21(DE3) (Novagen) for protein expression. HC-BoNT/B-pRESTa was transformed into BL21(DE3)pLysS (Thermo Fischer Scientific) for protein expression.

Purification of recombinant HC-BoNTs. *E.coli* BL21(DE3) HC-BoNT/A5-pET28a+ and HC-BoNT/D-pET28a+, were grown overnight on LB plates with 50μg/ml kanamycin and preinoculated into LB medium (20 ml) containing the same antibiotic 37°C overnight. The preculture was then inoculated into LB medium (1:50) containing kanamycin. The cells were grown at 37°C for 2 h at 200 rpm to an optical density of 0.6-0.8. Protein expression was induced with 1mM isopropyl-1-thio-β-D-galactopyranoside (IPTG) and followed by on overnight culture at 16°C under continuous shaking. The cells were harvested by centrifugation at 5000 rpm for 15 min, and the cell pellet was resuspended in the following lysis buffer: 20mM Tris-HCl (pH 7.6), 500mM NaCl, 10mM Imidazole, EDTA-free protease inhibitor (Roche), 1 mg/ml lysozyme, DNase, 1mM PMSF, 5% glycerol. After 1h incubation

with the lysis buffer at 4°C the cells were sonicated. The crude lysate was clarified by centrifugation at 22000 rpm for 45 min at 4°C and filtration through a 0.45 μm membrane filter. The supernatant was loaded onto a prepacked HisTrap Ni column (GE Healthcare) equilibrated with 20mM Tri-HCl (pH 7.6), 500mM NaCl, 10mM imidazole. After loading the column was washed with 20mM Tri-HCl (pH 7.6), 500mM NaCl, 20mM imidazole, for about 10 column volume. The protein was eluted over a 0-500 mM imidazole gradient in the same buffer. The fractions containing the protein were pooled, concentrated and further purified by size-exclusion chromatography using a Superdex 200, 10/300GL column (GE Healthcare), pre-equilibrated with 20 mM Tris-HCl pH 7.4; 150 mM NaCl. The pure protein fractions were pooled and concentrated using 30 kDa cutoff membrane filter (Amicon Millipore). The final concentration of the proteins was determined by absorption spectroscopy at 280 nm. The samples of each purification step are analysed for their purity on 4-12% NuPage (Life Technologies). Protein identity was confirmed by Western Blotting using an anti-His tag antibody (Novagen, 1:1000) .

The same expression and purification protocol was used also for the HC-BoNT/B.

Immunoblotting. For immunoblotting analysis equal amounts of protein were loaded onto a 4-12% NuPage gel and separated by electrophoresis in MES buffer (Life technologies). Proteins were then transferred onto Protran nitrocellulose membranes (Whatman) and saturated for 1 h in PBST (PBS 0.1% Tween20) supplemented with 5% non-fatty milk.in Incubation with primary antibodies was performed overnight at 4°C. The membranes were then washed three times with PBST and incubated with secondary HRP-conjugated antibodies. Finally, membranes were washed three times with PBST and twice with PBS. Visualization was carried out using Luminata Crescendo (Merck Millipore).

Neuronal culture. Primary cultures of rat cerebellar granule neurons (CGNs) were prepared from 6- to 8-days-old rats. Cerebella were isolated, mechanically disrupted and then trypsinized in the presence of DNase I. Cells were then plated into 24 well plates, pre-coated with poly-L-lysine (50 μg/mL), at a cell density of 4 x 105 cells per well. Cultures were maintained at 37 °C, 5% CO_2, 95% humidity in BME supplemented with 10% fetal bovine serum, 25 mM KCl, 2 mM glutamine and 50 μg/mL gentamicin (indicated as complete culture medium). To arrest growth of non-neuronal cells, cytosine arabinoside (10 μM) was added to the medium 18–24 h after plating.

HC-BoNTs binding and internalization into neurons. CGNs ate 6-8 DIV were washed in phosphate-buffered saline (PBS) and incubated with 200 nM of each HcBoNT in 500 µl buffer (15 mM HEPES, 145 mM NaCl, 2.2 mM $CaCl_2$, 0.5 mM $MgCl_2$, pH 7.4) supplemented with either low potassium (5.6 mM KCl) or high potassium (56 mM KCl) for 1 h at 37°C and 5% CO_2. After the treatment, CGNs were then washed (3X) with PBS, fixed for 10 minutes at RT with 4% paraformaldehyde in PBS, and then quenched (50 mM NH_4Cl in PBS) for 20 minutes. They were directly imaged or permeabilized and stained with a primary antibody specific for the fluorescent tag of each HC. For immunofluorescence, cells were permeabilized with 0.1% (v/v) TritonX-100 in PBS for 15 minutes at RT, and washed (3X) in PBS. Then were blocked in 10% (vol/vol) fetal bovine serum, 2.5% (wt/vol) cold fish skin gelatin, 0.1% Triton X-100, 0.05% Tween 20 in PBS, and the primary antibody rabbit α-GFP (Cell Signaling, 1:1000), was incubated overnight at 4°C in 5% (vol/vol) fetal bovine serum, 1% (wt/vol) cold fish skin gelatin, 0.1% Triton X-100, and 0.05% Tween 20 in DPBS. Cells were washed 3 times and incubated for 1 h with the secondary antibody goat α-rabbit Alexa Flour- 488 (Life Technologies, 1:200). Washed again (3X) with PBS. Then coverslips were mounted using Fluorescent Mounting Medium (Dako, S3023) and examined by confocal Leica SP5. Images were collected with the same lamp intensity and exposure time.

In vivo injection of HC-BoNTs and NMJ Immunohistochemistry. For in vivo experiments, adult mice CD1/Swiss-Webster weighing 26-28g, were anesthetized with isoflurane, followed by injection of HcBoNTs (1 µg) in proximity of the LAL muscle. After 10 minutes the mice were sacrificed, LAL muscle dissected and fixed in 4% (wt/vol) PFA in PBS for 30 min at RT. Samples were quenched and washed (3X) with PBS, before staining for 30 minutes at RT with Alexa Flour-555 conjugated α-bungarotoxin (Invitrogen B3545, 1:200). Neuromuscular junctions were analysed with a Leica SP5 confocal microscope equipped with a 63× HCX PL APO NA 1.4. Laser excitation line, power intensity, and emission range were chosen according to each fluorophore of BoNTs.

4. RESULTS AND DISCUSSION

Expression and purification of the BoNT-HCs. Synthetic genes encoding *E. coli* codon-optimized cpYFP-HC-BoNT/A5 (residues 876-1296); mCherry-HC-BoNT/D (residues 863-1276); GFP-HC-BoNT/B (residues 832-1290) were synthesized at the indicated source. The synthesized DNA was further successfully subcloned into an appropriate expression vector. Protein expression of each HC in *E. coli* BL21(DE3) for BoNT/A5 and /D, and BL21(DE3)pLysS for BoNT/B was optimized by titration of induction temperature and IPTG concentration. Purification protocols were developed for each HC-BoNT serotype by adjusting the purification temperature and ionic strength of the buffers in the chromatography steps. The three different fluorescent tags (cpYFP, mCherry and GFP) were chosen in order to visualize the HC also in experiments of co-incubation and co-injection. *E.coli* produced HC-BoNT/A5/D and /B as soluble ~80 kDa, ~76 kDa, ~83 kDa proteins respectively (Molecular weights are calculated considering also the fluorescent tag of each HC-BoNT). While the overall expression levels of the three serotypes of HCRs in *E. coli* were similar, differences in final yields were due primarily to the differential solubility of the HC-BoNTs when extracted from the cell lysates (>90% for HC-A5 and HC-D to ~15% for HC-B). The two-step purification, utilizing affinity chromatography and gel filtration, was sufficient to yield purifications of each HCR to >80% purity, as detected by SDS-page analysis. Western blot analysis against the N-terminal 6xHis tag of each HC-BoNT confirmed the protein identity (Figure 4.1, B and C). The final yield of soluble HCs ranged from ~2 to 10 mg in batch culture.
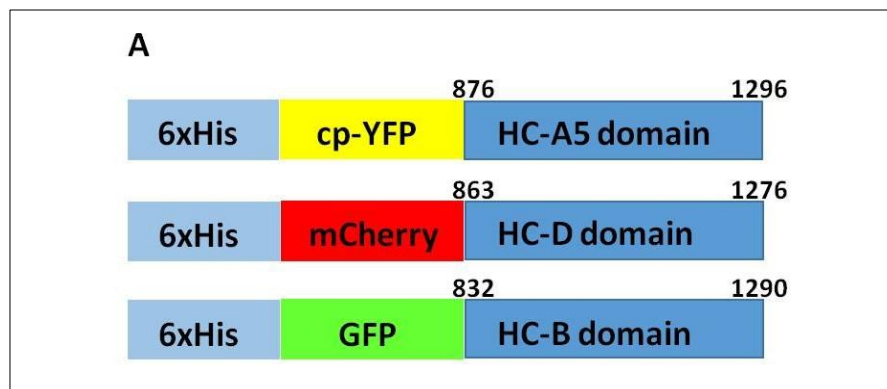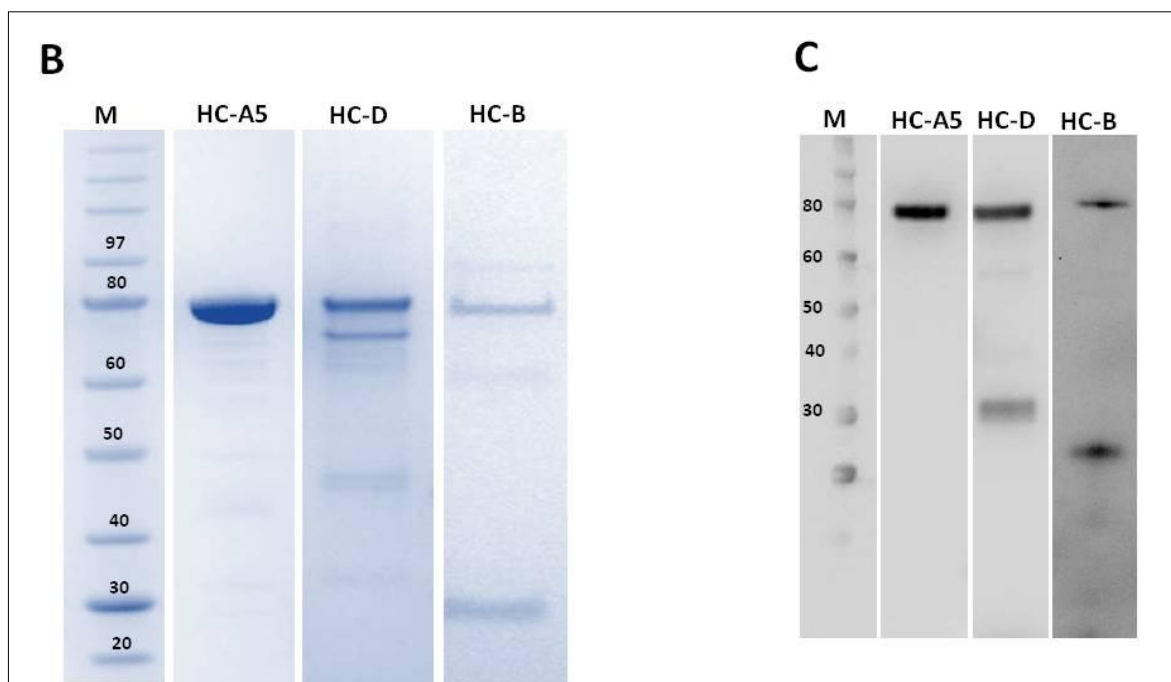
Fig. 4.1: Purification of HC-BoNT/A5/D and /B. (A) Ribbon diagram of the HC-BoNTs prepared for this work. They were expressed as 6-His-tag fusion proteins in *E. coli*. Proteins were purified by affinity- and size-exclusion chromatography. (B) Five micrograms of each HCR was subjected to sodium dodecyl sulfate-polyacrylamide gel electrophoresis. The gel was stained with Coomassie blue and is shown. To the left are the migrations of three molecular size markers (kDa). (C) Western blot analysis using anti His tag antibody in order to identify the proteins purified.

Binding and internalization of the HC-BoNTs into neuronal cells. The first step of the cellular intoxication mechanism is the specific binding of BoNTs to peripheral nerve endings, followed by their internalization via endocytosis into not well identified vesicular compartments for the BoNT serotypes. To better investigate this step, we took advantage of the binding domains, that fully maintain the capability of parental BoNTs, to bind to the presynaptic membrane of neurons and to be endocytosed. The use of cultures cerebellum granular neurons (CGNs) offers a simple and a rapid way to test the specificity and functionality of the prepared recombinant binding domains of BoNT serotypes. The 1 h incubation with 200 nM of each HC-BoNT at 37°C, gave a high specific staining at the axon of the neuronal cells, compared to the controls in which CGNs were in incubated with 200 nM recombinant GFP and mCherry (Figure 4.2, A). Interestingly, the three HCs used, display clearly different patterns of staining, suggesting that they may be internalized inside different compartments (Figure 4.2, B).
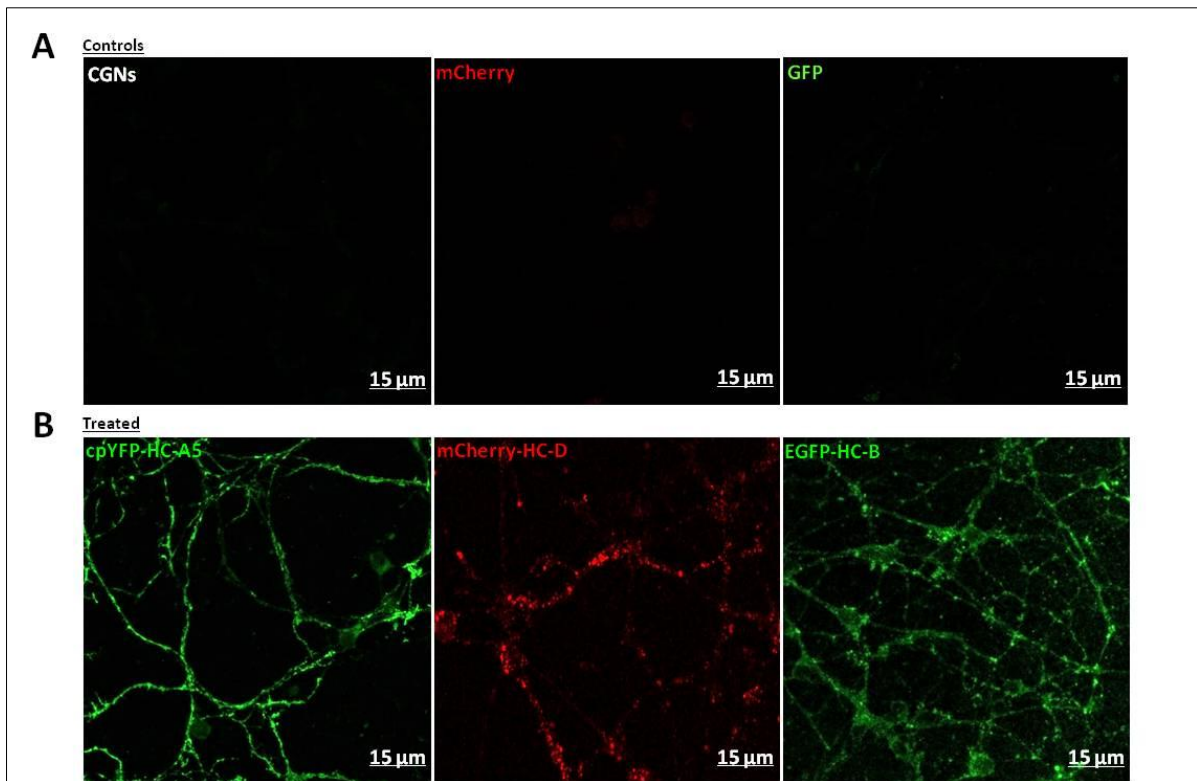
Fig. 4.2: Immuncytochemical alanalysis of HC-BoNT/A5/D and /B in CGNs. (A) untreated CGNs as control, and CGNs treated with 200 nM of each fluorophore: GFP and mCherry. (B) CGNs were treated with 200 nM of each HC-BoNT at 37 °C for 1 h. Samples were fixed and directly stained for all the three HCs. The images shown are representative of three independent experiments. Scale bar, 15 μm.

Binding and internalization of the HC-BoNTs into the neuromuscular junction. After we validated in vitro the specificity of the prepared HCs, we carried out *in vivo* experiments at the neuromuscular junction, the site of action of BoNTs. 1 μg of each HC-BoNT was injected near the level of the LAL muscle, and then analysed for the staining of NMJs. The images of this analysis, are shown in Figure 4.3. They clearly indicate, that the HCs label only motor nerve terminals within the boundaries defined by the pos-synaptic nicotinic acetylcholine receptor, visualized here by the very specific binding of fluorescent α- BTX. Thus, the recombinant HCs fully maintain the capability of parental BoNTs. The NMJ staining clearly shows that the HC binding is restricted to the presynaptic membrane. However, the level of resolution of this analysis does not allow us to distinguish toxin bound to the nerve terminal surface from the one internalized.
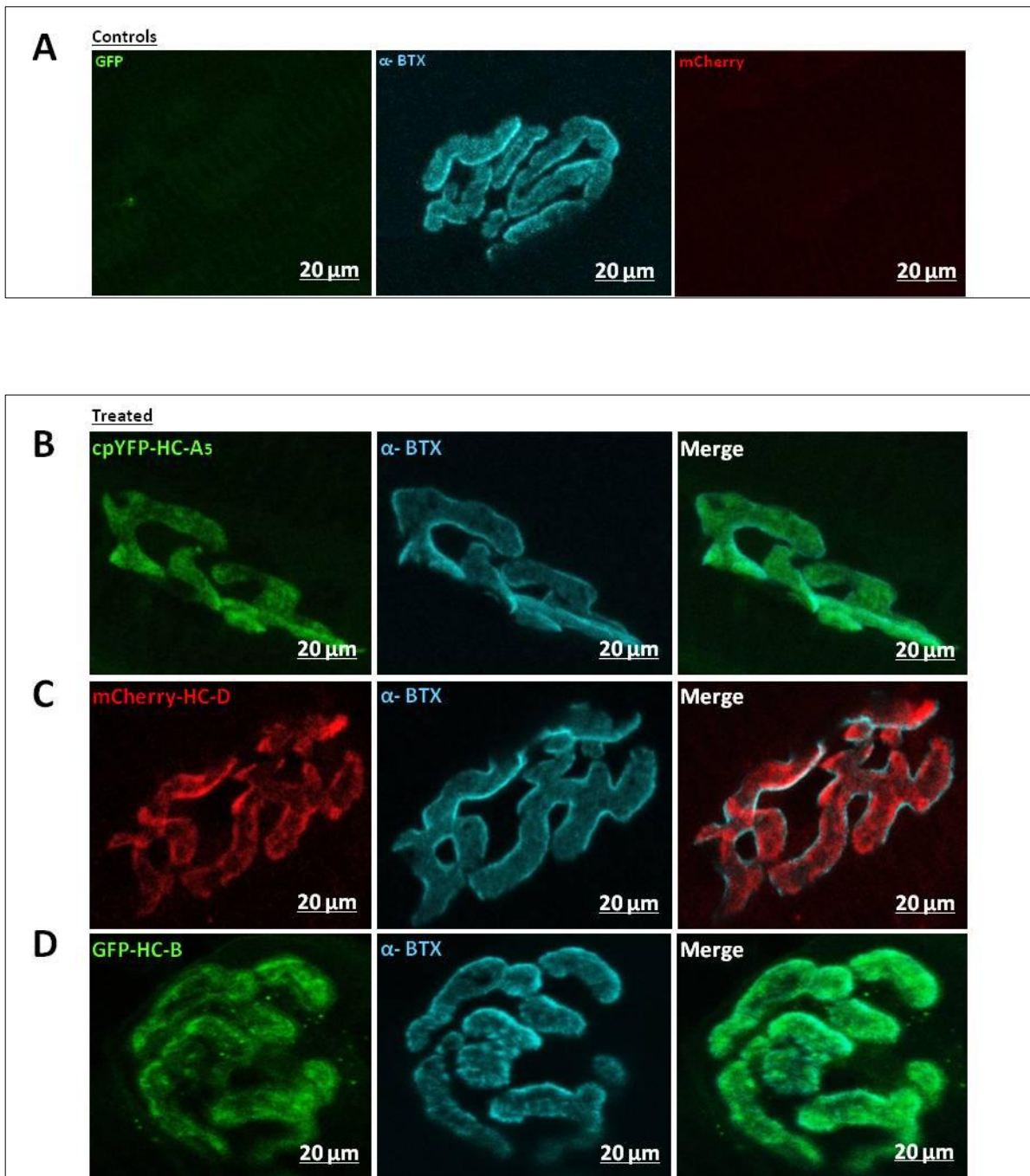
Fig. 4.3: The NMJ stained with HC-BoNT/A5/D and /B. The botulinum neurotoxin binding domains bind to the axon terminal of the mouse NMJ, as shown by confocal fluorescent microscopy. A top view of four different NMJs revealed by the staining of the post-synaptic acetylcholine receptors with Alexa 555-labeled α-bungarotoxin (α-BTX). (A) NMJ as control, and from mice injected with 1 µg each fluorophore: GFP and mCherry, as control for aspecific binding (B) NMJ stained HC-BoNT/A5. Showing cpYFP fluorescence distributed along the motor nerve terminal and restricted to the NMJ defined by the α-BTX s staining. (C) and (D) The same for the NMJ stained with mCherry-HC-D and GFP-HCB. Side view of the NMJs clearly shows that the labeling from each HC-BoNT is mainly found at the presynaptic side of the nerve terminal e does not co-localize with α-BTX (Merge). The images shown are from three independent experiments. Scale bar, 20 µm.

In vivo co-injection of two different HC-BoNTs: the HC-A5 and HC-D at the level of the LAL muscle. Considering that the HC-BoNTs are conjugated with different fluorophores, we can evaluate their different staining by co-injection and directly visualize their staining through fluorescent microscopy. Again 1 μg of cpYFP-HC-BoNT/A5 and 1 μg of mCherry-HC-BoNT/D, were co-injected at the level of LAL muscle. After 10 minutes the muscle was dissected and the NMJs analysed at confocal microscope. The images are shown in Figure 4.4. They clearly indicate a complete co-localization of the two different HC-BoNTs, as we can appreciate from the immunoflourescent staining. It seems as the two BoNTs have the same initial trafficking pathway at the NMJ and bind the same protein receptor. However, further analysis are required to better confirm this data.

Fig. 4.4: The NMJ stained with HC-BoNT/A5 and /D. A top view of the NMJ stained with 1 μg of cp-YFP-HC-BoNT/A5 and 1 μg mCherry-HC-BoNT/D. Side view of the NMJs clearly shows that the labeling from each HC-BoNT is mainly found at the presynaptic side of the nerve terminal and completely co-localize with each other. The images shown are from three independent experiments. Scale bar, 20 μm.

In vivo co-injection of two different HC-BoNTs: the HC-B and HC-D at the level of the LAL muscle. We then performed another co-injection experiment with the two other HC-BoNTs: GFP-HC-BoNT/B and mCherry-HC-BoNT/D. The experiments was perfomed as previously explained for the co-injection of the other couple of HCs. Again, images are shown in Figure 4.5. In this case they indicate a partial co-localization of the two HC-BoNTs tested. The staining seems to be different for the two BoNTs. As reported, BoNT/B and BoNT/D have different time required for intoxication and due to this they may follow a different pathway for their trafficking. Anyway, the experiment was performed just at one timepoint, 10 minutes. It would be interesting to further investigate this difference also at other timepoints.
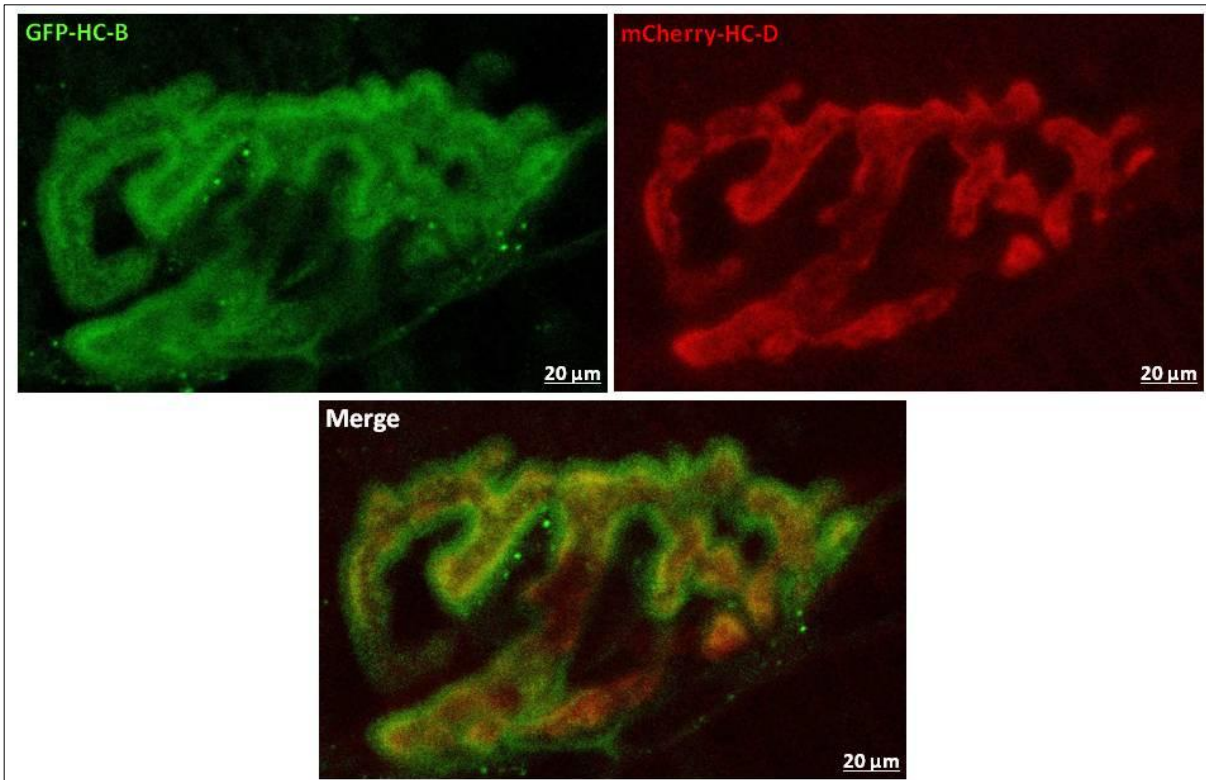
Fig. 4.5: The NMJ stained with HC-BoNT/B and /D. A top view of the NMJ stained with 1 µg of GFP-HC-BoNT/B and 1 µg mCherry-HC-BoNT/D. Side view of the NMJs clearly shows that the labeling from each HC-BoNT is mainly found at the presynaptic side of the nerve terminal and partially co-localize with each other. The images shown are from three independent experiments. Scale bar, 20 µm.

5. CONCLUSIONS

The high potency of BoNTs is mainly due to their neurospecific binding at the level of the peripheral nerve terminal which mediated by the interaction with two receptor components. All BoNTs bind first to gangliosides abundantly present on neuronal membranes. Then, upon endocytosis they reach their protein receptor, different for each BoNT serotype. The cell binding is mediated by the 50 kDa HC-domain. The N-terminal HC mediates the binding with the gangliosides, instead the C-terminal HC mediates the one with the protein receptor. BoNT/B, BoNT/G and BoNT/DC bind with their HC- domain to the lumenal domain of synaptotagmin-I/II (Syt-I, Syt-II). By contrast, BoNT/A and BoNT/E bind specifically to two different segments of the fourth lumenal loop of the synaptic vesicle transmembrane protein SV2. The protein receptors of other BoNTs have not been yet fully characterized, although SV2 seems to play an important role in the uptake mechanism of BoNT/D and BoNT/F. The known BoNT receptors are in the luminal domain of synaptic vesicles strongly suggests that BoNTs are endocytosed inside synaptic vesicles at peripheral nerve terminals. However, their actual presence inside vesicles and the type of synaptic vesicles have not been determined.

This part of my thesis work, aimed in studying the initial trafficking pathway of BoNT serotypes at the level of the neuromuscular junction (NMJ). The most important informations delivered by my work are: i) the recombinant binding domain of BoNTs (HC-BoNTs) are ideal tools to exploit the initial trafficking pathways. They are both necessary and sufficient for binding to the neuronal surface and internalization. I demonstrated *in vitro* and *in vivo*, that this property is completely conserved since they label in a very specific way only motor nerve terminals; ii) the NMJ fluorescent staining with HC-BoNT/A5 and mCherry-HC-D clearly show a complete co-localization of the two proteins, supporting the hypothesis of the same protein receptor for BoNT/A5 and BoNT/D. Therefore, in agreement with several published data (Peng *et al.,* 2011; Rummel, 2015); iii) Instead, the fluorescent staining of NMJ with GFP-HC-BoNT/B and mCherry-HC-D show a partial co-localization of the two proteins. Supporting the fact that the time required for the intoxication is different for BoNT/B and BoNT/D, thus they may follow a different vesicular trafficking. However, further analysis are required to better clarify the distribution of BoNTs at the NMJ, in particular high resolution techniques such as electron microscopy.

6. REFERENCES

1. Gill DM. Bacterial toxins: a table of lethal amounts. Microbiological Reviews.1982; 46(1): 8694.

2. Rossetto O, Pirazzini M, Montecucco C. Botulinum neurotoxins: genetic, structural and mechanistic insights. Nat Rev Microbiol. 2014.

3. Rummel A. The long journey of botulinum neurotoxins into the synapse. Toxicon. 2015; 107(Pt A): 9-24.

4. Montecucco C. How do tetanus and botulinum toxins bind to neuronal membranes? Trends in biochemical sciences. 1986; 11(8): 314-317.

5. Binz T, Rummel A. Cell entry strategy of clostridial neurotoxins. J Neurochem. 2009; 109(6): 1584-1595.

6. Brunger AT, Rummel A. Receptor and substrate interactions of clostridial neurotoxins. Toxicon. 2009; 54(5): 550-560.

7. Rummel A. Double receptor anchorage of botulinum neurotoxins accounts for their exquisite neurospecificity. Curr Top Microbiol Immunol. 2013; 364: 61-90.

8. Muraro L, Tosatto S, Motterlini L, Rossetto O, Montecucco C. The N-terminal half of the receptor domain of botulinum neurotoxin A binds to microdomains of the plasma membrane. Biochem Biophys Res Commun. 2009; 380(1): 76-80.

9. Zhang Y, Varnum SM. The receptor binding domain of botulinum neurotoxin serotype C binds phosphoinositides. Biochimie. 2012; 94(3): 920-923.

10. Ayyar BV, Aoki KR, Atassi MZ. The C-terminal heavy-chain domain of botulinum neurotoxin a is not the only site that binds neurons, as the N-terminal heavy-chain domain also plays a very active role in toxin-cell binding and interactions. Infect Immun. 2015;83(4):1465-1476.

11. Fischer A, Montal M. Single molecule detection of intermediates during botulinum neurotoxin translocation across membranes. Proc Natl Acad Sci U S A. 2007; 104(25): 10447-10452.

12. Montal M. Botulinum neurotoxin: a marvel of protein design. Annu Rev Biochem. 2010; 79: 591-617.

13. Pirazzini M, Tehran DA, Leka O, Zanetti G, Rossetto O, Montecucco C. On the translocation of botulinum and tetanus neurotoxins across the membrane of acidic intracellular compartments. Biochim Biophys Acta. 2016 Mar; 1858(3): 467-74.

14. Pantano S, Montecucco C. The blockade of the neurotransmitter release apparatus by botulinum neurotoxins. Cell Mol Life Sci. 2013.

15. Matteoli M, Verderio C, Rossetto O, et al. Synaptic vesicle endocytosis mediates the entry of tetanus neurotoxin into hippocampal neurons. Proc Natl Acad Sci U S A. 1996; 93(23): 13310-13315.

16. Ledeen RW, Diebler MF, Wu G, Lu ZH, Varoqui H. Ganglioside composition of subcellular fractions, including pre- and postsynaptic membranes, from Torpedo electric organ. Neurochem Res. 1993; 18(11): 1151-1155.

17. Sonnino S, Mauri L, Chigorno V, Prinetti A. Gangliosides as components of lipid membrane domains. Glycobiology. 2007; 17(1): 1R-13R.

18. Karalewitz AP, Kroken AR, Fu Z, Baldwin MR, Kim JJ, Barbieri JT. Identification of a unique ganglioside binding loop within botulinum neurotoxins C and D-SA. Biochemistry. 2010; 49(37): 8117-8126.

19. Strotmeier J, Lee K, Volker AK, et al. Botulinum neurotoxin serotype D attacks neurons via two carbohydrate-binding sites in a ganglioside-dependent manner. Biochem J. 2010; 431(2): 207-216.

20. Zhang Y, Buchko GW, Qin L, Robinson H, Varnum SM. Crystal structure of the receptor binding domain of the botulinum C-D mosaic neurotoxin reveals potential roles of lysines 1118 and 1136 in membrane interactions. Biochem Biophys Res Commun. 2011; 404(1): 407-412.

21. Karalewitz AP, Fu Z, Baldwin MR, Kim JJ, Barbieri JT. Botulinum neurotoxin serotype C associates with dual ganglioside receptors to facilitate cell entry. J Biol Chem. 2012; 287(48): 40806-40816.

22. Nishiki T, Kamata Y, Nemoto Y, et al. Identification of protein receptor for Clostridium botulinum type B neurotoxin in rat brain synaptosomes. J Biol Chem. 1994; 269(14): 10498-10503.

23. Nishiki T, Tokuyama Y, Kamata Y, et al. The high-affinity binding of Clostridium botulinum type B neurotoxin to synaptotagmin II associated with gangliosides GT1b/GD1a. FEBS Lett. 1996; 378(3): 253-257.

24. Dong M, Richards DA, Goodnough MC, Tepp WH, Johnson EA, Chapman ER. Synaptotagmins I and II mediate entry of botulinum neurotoxin B into cells. J Cell Biol. 2003; 162(7): 1293-1303.

25. Rummel A, Karnath T, Henke T, Bigalke H, Binz T. Synaptotagmins I and II act as nerve cell receptors for botulinum neurotoxin G. J Biol Chem. 2004; 279(29): 30865-30870.

26. Mahrhold S, Rummel A, Bigalke H, Davletov B, Binz T. The synaptic vesicle protein 2C mediates the uptake of botulinum neurotoxin A into phrenic nerves. FEBS Lett. 2006; 580(8): 2011-2014.

27. Chai Q, Arndt JW, Dong M, et al. Structural basis of cell surface receptor recognition by botulinum neurotoxin B. Nature. 2006; 444(7122): 1096-1100.

28. Jin R, Rummel A, Binz T, Brunger AT. Botulinum neurotoxin B recognizes its protein re8ceptor with high affinity and specificity. Nature. 2006; 444(7122): 1092-1095.

29. Dong M, Tepp WH, Liu H, Johnson EA, Chapman ER. Mechanism of botulinum neurotoxin B and G entry into hippocampal neurons. J Cell Biol. 2007; 179(7): 1511-1522.

30. Peng L, Berntsson RP, Tepp WH, et al. Botulinum neurotoxin D-C uses synaptotagmin I and II as receptors, and human synaptotagmin II is not an effective receptor for type B, D-C and G toxins. J Cell Sci. 2012; 125(Pt 13): 3233-3242.

31. Berntsson RP, Peng L, Svensson LM, Dong M, Stenmark P. Crystal Structures of Botulinum Neurotoxin DC in Complex with Its Protein Receptors Synaptotagmin I and II. Structure. 2013; 21(9): 1602-1611.

32. Willjes G, Mahrhold S, Strotmeier J, Eichner T, Rummel A, Binz T. Botulinum neurotoxin G binds synaptotagmin-II in a mode similar to that of serotype B: tyrosine 1186 and lysine 1191 cause its lower affinity. Biochemistry. 2013; 52(22): 3930-3938.

33. Dong M, Yeh F, Tepp WH, et al. SV2 is the protein receptor for botulinum neurotoxin A. Science. 2006; 312(5773): 592-596.

34. Dong M, Liu H, Tepp WH, Johnson EA, Janz R, Chapman ER. Glycosylated SV2A and SV2B mediate the entry of botulinum neurotoxin E into neurons. Mol Biol Cell. 2008;19(12):5226-5237.

35. Benoit RM, Frey D, Hilbert M, et al. Structural basis for recognition of synaptic vesicle protein 2C by botulinum neurotoxin A. Nature. 2014; 505(7481): 108-111.

36. Fu Z, Chen C, Barbieri JT, Kim JJ, Baldwin MR. Glycosylated SV2 and gangliosides as dual receptors for botulinum neurotoxin serotype F. Biochemistry. 2009; 48(24): 5631-5641.

37. Rummel A, Hafner K, Mahrhold S, et al. Botulinum neurotoxins C, E and F bind gangliosides via a conserved binding site prior to stimulation-dependent uptake with botulinum neurotoxin F utilising the three isoforms of SV2 as second receptor. J Neurochem.

2009; 110(6): 1942-1954.

38. Peng L, Tepp WH, Johnson EA, Dong M. Botulinum neurotoxin D uses synaptic vesicle protein SV2 and gangliosides as receptors. PLoS Pathog. 2011;7(3):e1002008. doi: 1002010.1001371/journal.ppat.1002008.

39. Colasante C, Rossetto O, Morbiato L, Pirazzini M, Molgo J, Montecucco C. Botulinum neurotoxin type A is internalized and translocated from small synaptic vesicles at the neuromuscular junction. Mol Neurobiol. 2013; 48(1): 120-127.

40. Pellett S, Tepp WH, Scherf JM, Johnson EA. Botulinum Neurotoxins Can Enter Cultured Neurons Independent of Synaptic Vesicle Recycling. PLoS ONE. 2015; 10(7): e0133737.

41. Sudhof TC. Neurotransmitter release: the last millisecond in the life of a synaptic vesicle. Neuron. 2013; 80(3): 675-690.

42. Simpson LL, Coffield JA, Bakry N. Inhibition of vacuolar adenosine triphosphatase antagonizes the effects of clostridial neurotoxins but not phospholipase A2 neurotoxins. J Pharmacol Exp Ther. 1994; 269(1): 256-262.

43. Sun S, Tepp WH, Johnson EA, Chapman ER. Botulinum neurotoxins B and E translocate at different rates and exhibit divergent responses to GT1b and low pH. Biochemistry. 2012; 51(28): 5655-5662.

44. Koriazova LK, Montal M. Translocation of botulinum neurotoxin light chain protease through the heavy chain channel. Nat Struct Biol. 2003; 10(1): 13-18.

45. Fischer A, Montal M. Molecular dissection of botulinum neurotoxin reveals interdomain chaperone function. Toxicon. 2013 Dec 1; 75: 101-7.

46. Fischer A, Montal M. Crucial role of the disulfide bridge between botulinum neurotoxin light and heavy chains in protease translocation across membranes. J Biol Chem. 2007; 282(40): 29604-29611.

47. Fischer A, Nakai Y, Eubanks LM, et al. Bimodal modulation of the botulinum neurotoxin protein-conducting channel. Proc Natl Acad Sci U S A. 2009; 106(5): 1330-1335.

48. Kukreja R, Singh B. Biologically active novel conformational state of botulinum, the most poisonous poison. J Biol Chem. 2005; 280(47): 39346-39352.

49. Cai S, Kukreja R, Shoesmith S, Chang TW, Singh BR. Botulinum neurotoxin light chain refolds at endosomal pH for its translocation. Protein J. 2006; 25(7-8): 455-462.

50. Galloux M, Vitrac H, Montagner C, et al. Membrane Interaction of botulinum neurotoxin A translocation (T) domain. The belt region is a regulatory loop for membrane interaction. J

Biol Chem. 2008; 283(41): 27668-27676.

51. Eswaramoorthy S, Kumaran D, Keller J, Swaminathan S. Role of Metals in the Biological Activity of Clostridium botulinum Neurotoxins†,‡. Biochemistry. 2004; 43(8): 2209-2216.

52. Sun S, Suresh S, Liu H, et al. Receptor binding enables botulinum neurotoxin B to sense low pH for translocation channel assembly. *Cell Host Microbe.* 2011; 10(3): 237-247.

53.Montecucco C, Schiavo G, Dasgupta BR. Effect of pH on the interaction of botulinum neurotoxins A, B and E with liposomes. Biochem J. 1989; 259(1): 47-53.

54. Fu FN, Busath DD, Singh BR. Spectroscopic analysis of low pH and lipid-induced structural changes in type A botulinum neurotoxin relevant to membrane channel formation and translocation. Biophys Chem. 2002; 99(1): 17-29.

55. Puhar A, Johnson EA, Rossetto O, Montecucco C. Comparison of the pH-induced conformational change of different clostridial neurotoxins. Biochem Biophys Res Commun. 2004;319(1):66-71.

56. Pirazzini M, Rossetto O, Bolognese P, Shone CC, Montecucco C. Double anchorage to the membrane and intact inter-chain disulfide bond are required for the low pH induced entry of tetanus and botulinum neurotoxins into neurons. Cell Microbiol. 2011;13(11):1731-1743.

57. Pirazzini M, Henke T, Rossetto O, Mahrhold S, Krez N, Rummel A, Montecucco C, Binz T. Neutralisation of specific surface carboxylates speeds up translocationof botulinum neuro-toxin type B enzymatic domain. FEBS Lett. 2013 Nov 29; 587(23): 3831-6.

58. Schiavo G, Papini E, Genna G, Montecucco C. An intact interchain disulfide bond is re-quired for the neurotoxicity of tetanus toxin. Infect Immun. 1990; 58(12): 4136-4141.

59. Pirazzini M, Tehran DA, Zanetti G, Lista F, Binz T, Shone CC, Rossetto O, Montecucco C. The thioredoxin reductase--Thioredoxin redox system cleaves the interchain disulphide bond of botulinum neurotoxins on the cytosolic surface of synaptic vesicles. Toxicon. 2015 Dec 1;107(Pt A):32-6.

60. Arner ES, Holmgren A. Physiological functions of thioredoxin and thioredoxin reductase. Eur J Biochem. 2000;267(20):6102-6109.

61. Hanschmann EM, Godoy JR, Berndt C, Hudemann C, Lillig CH. Thioredoxins, glutaredoxins, and peroxiredoxins-molecular mechanisms and health significance: from cofactors to antioxidants to redox signaling. Antioxid Redox Signal. 2013; 19(13): 1539-1605.

62. Holmgren A, Lu J. Thioredoxin and thioredoxin reductase: current research with special reference to human disease. Biochem Biophys Res Commun. 2010; 396(1): 120-124.

63. Powis G, Kirkpatrick DL. Thioredoxin signaling as a target for cancer therapy. Curr Opin Pharmacol. 2007; 7(4): 392-397.

64. Pirazzini M, Bordin F, Rossetto O, Shone CC, Binz T, Montecucco C. The thioredoxin reductase-thioredoxin system is involved in the entry of tetanus and botulinum neurotoxins in the cytosol of nerve terminals. FEBS Lett. 2013; 587(2): 150-155.

65. Pirazzini M, Azarnia Tehran D, Zanetti G, Megighian A, Scorzeto M, Fillo S,Shone CC, Binz T, Rossetto O, Lista F, Montecucco C. Thioredoxin and its reductase are present on synaptic vesicles, and their inhibition prevents the paralysis induced by botulinum neurotoxins. Cell Rep. 2014 Sep 25; 8(6): 1870-8.

67. Schiavo G, Santucci A, Dasgupta BR, Mehta PP, Jontes J, Benfenati F, Wilson MC, Montecucco C. Botulinum neurotoxins serotypes A and E cleave SNAP-25 at distinct COOH-terminal peptide bonds. FEBS Lett. 1993 Nov 29; 335(1): 99-103.

68. Blasi J, Chapman ER, Link E, Binz T, Yamasaki S, De Camilli P, Südhof TC, Niemann H, Jahn R. Botulinum neurotoxin A selectively cleaves the synaptic protein SNAP-25. Nature. 1993 Sep 9; 365(6442): 160-3.

69. Schiavo G, Benfenati F, Poulain B, Rossetto O, Polverino de Laureto P, DasGupta BR, Montecucco C. Tetanus and botulinum-B neurotoxins block neurotransmitter release by proteolytic cleavage of synaptobrevin. Nature. 1992 Oct 29; 359(6398): 832-5.

Schiavo G, Rossetto O, Catsicas S, Polverino de Laureto P, DasGupta BR, Benfenati F, Montecucco C. Identification of the nerve terminal targets of botulinum neurotoxin serotypes A, D, and E. J Biol Chem. 1993 Nov 15; 268(32): 23784-7.

70. Sutton RB, Fasshauer D, Jahn R, Brunger AT. Crystal structure of a SNARE complex involved in synaptic exocytosis at 2.4 A resolution. Nature. 1998; 395(6700): 347-353.

71. Schiavo G, Matteoli M, Montecucco C. Neurotoxins affecting neuroexocytosis. Physiol Rev. 2000; 80(2): 717-766.

72. Binz T. Clostridial neurotoxin light chains: devices for SNARE cleavage mediated blockade of neurotransmission. Curr Top Microbiol Immunol. 2013; 364: 139-157.

PUBBLICATIONS LIST

- Zornetta I, Azarnia Tehran D, Arrigoni G, Anniballi F, Bano L, **Leka O**, Zanotti G, Binz T, Montecucco C. The first non Clostridial botulinum-like toxin clave VAMP within the juxtamembrane domain. Sci Rep. 2016 Jul 22.

- Azarnia Tehran D, Pirazzini M, **Leka O**, Mattarei A, Lista F, Binz T, Rossetto O, Montecucco C. Hsp90 is involved in the entry of Clostridial Neurotoxins into the Cytosol of Nerve Terminals. Cell Microbiol. 2016 Jul 12.

- Azarnia Tehran D, Zanetti G, **Leka O**, Lista F, Fillo S, Binz T, Shone CC, Rossetto O, Montecucco C, Paradisi C, Mattarei A, Pirazzini M. A Novel Inhibitor Prevents the Peripheral Neuroparalysis of Botulinum Neurotoxins. Sci Rep. 2015 Dec 16.

- Pirazzini M, Tehran DA, **Leka O**, Zanetti G, Rossetto O, Montecucco C. On the translocation of botulinum and tetanus neurotoxins across the membrane of acidic intracellular compartments. Biochim Biophys Acta. 2016 Mar.

- **Leka O**, Vallese F, Pirazzini M, Berto P, Montecucco C, Zanotti G. Diphtheria toxin conformational switching at acidic pH. FEBS J. 2014 May.

ACKNOWLEDGEMENTS